SiGe HBTs
Operating at Deep Cryogenic Temperatures

A Thesis

by

Jiahui Yuan

Submitted to the Reading Committee
In Partial Fulfillment of the Requirements for the
Degree Master of Science

Master Thesis Advisor

Dr. John D. Cressler

School of Electrical and Computer Engineering
Georgia Institute of Technology
Atlanta, GA 30332

May, 2007

SiGe HBTs
Operating at Deep Cryogenic Temperatures

Approved by:

Professor John D. Cressler, Advisor
School of Electrical and Computer Engineering
Georgia Institute of Technology

Professor Joy Laskar
School of Electrical and Computer Engineering
Georgia Institute of Technology

Professor Ioannis Papapolymerou
School of Electrical and Computer Engineering
Georgia Institute of Technology

Professor Paul D. Yoder
School of Electrical and Computer Engineering
Georgia Institute of Technology

Date Approved: May 6, 2007

ACKNOWLEDGEMENTS

I am really grateful for all those who provide me with the opportunity to complete this thesis. I would like to express my deepest gratitude to my advisor, Dr. John D. Cressler. Thank you for leading me into the magic world of microelectronics, for helping me get ready for the PhD work ahead, for educating me to take my responsibility, and for showing me the passion for life.

I would like to sincerely thank Dr. Joy Laskar, Dr. Ioannis Papapolymerou, Dr. Paul D. Yoder, who served as my reading committee members, for all their valuable comments and corrections on my thesis. Thank you to the members of the SiGe Devices and Circuits research team at Georgia Tech, especially Dr. E. Zhao, Dr. W. -M. L. Kuo, Dr. R. Krithivasan, Dr. B. Jun, Dr. B. Banerjee, Dr. J. Comeau, Dr. Y. Lu, Dr. A. P. Gnana Prakash, Dr. C. Zhu, Curtis, Akil, Marco, Laleh, Aravind, Tom, Steven, Kurt, Ryan, Gus, and Anuj. I would also like to extend my gratitude to Dr. G. Niu in Auburn University, Dr. Q. Liang in IBM, and Dr. Y. Cui in RFMD for all their instructions during the work of this thesis. This work could not have been accomplished without their significant contributions.

This work was mainly supported by NASA ETDP, under grants NNL05AA37C and NNL06AA29C, JPL, and the Georgia Electronic Design Center at Georgia Tech. I am grateful for the support of JPL, the IBM SiGe development group, as well the many contributions of the SiGe ETDP team.

Last, but most importantly, I want to thank my parents, Jie Yuan and Peilin Li, and my sister, Qingqing Yuan, who are always there supporting me. Thank you, family, for helping with the every step in my life. I sincerely thank my wife, Yueping Liu, for all all the emotional support ever since high school.

TABLE OF CONTENTS

LIST OF TABLES

LIST OF FIGURES

CHAPTER 1

INTRODUCTION

As Si-manufacturing compatible silicon-germanium heterojunction bipolar transistors (SiGe HBTs) are making rapid in-roads into RF through mm-wave circuit applications, with performance levels steadily marching upward, the use of these devices under extreme environment conditions are being studied extensively. In this work, test structures of SiGe HBTs were designed and put into extremely low temperatures, and a new negative differential resistance (NDR) effect and a novel collector current kink effect are investigated in the cryogenically-operated SiGe HBTs.

Theory based on an enhanced positive feedback mechanism associated with heterojunction barrier effect (HBE) at deep cryogenic temperatures is proposed to explain both the observed NDR and the collector current kink. The accumulated charge induced by the barrier effect acts at low temperatures to enhance the total collector current, indirectly producing both phenomena. This theory is confirmed using calibrated 2-D DESSIS simulations over temperature. These unique cryogenic effects also have significant impact on the *ac* performance of SiGe HBTs operating at high-injection. Technology evolution plays an important role in determining the magnitude of the observed phenomena, and the scaling implications are addressed. The input drive condition of the transistor during its use in circuits, either under pure forced-current bias or under pure forced-voltage bias, or more practically, somewhere in between, determines the magnitude of the observed NDR and is of potential concern for circuit designers and therefore must be carefully modeled.

Results from this thesis work has been presented at the IEEE Electron Device Meeting (IEDM) [1] and published on IEEE Transactions on Electron Devices [2].

1.1 SiGe HBTs

SiGe HBTs technology has emerged as an important alternative to III-V device technologies for RF and mixed-signal applications [3]. Commercial SiGe technologies were first developed at IBM over 20 years ago, and a tremendous growth has been shown in SiGe ever since. Transistor performance in the range of 50 - 100 GHz now exists in most of in many companies worldwide, while many high-performance circuits are now using the commercial 200-GHz SiGe HBTs made by the key SiGe players. Recent work has demonstrated that manufacturable SiGe HBT technologies with performance well above 300 GHz can be achieved by careful profile and structural design.

Table 1 summarizes the key performance parameters for SiGe technologies from IBM [4], [5]. Here the technologies 5HP/6HP, 7HP, 8HP, and 9T are typical representatives of the first-, second-, third-, and fourth-generation SiGe HBTs. The presence of Ge in the base region of a conventional Si BJT engineers the band structure of the device and greatly improves its operating speed to achieve that of the state-of-the-art III-V transistors (e.g. GaAs or InP). The enhancement in the frequency performance comes with only a modest compromise in the process complexity and the cost as compared to its Si BJTs counterpart. The cost-performance advantage has made SiGe HBT an extraordinary candidate for high-speed microwave and RF communication circuits. In addition, the ease of integrating SiGe HBTs with the dominant Si CMOS technology to form SiGe BiCMOS has provided further flexibility for circuit designs, where "system on a chip" becomes possible.

The superior performance of SiGe HBT over Si BJT is due to the bandgap engineering induced by the Ge (peak usually being 8-25%) in the base. This technique introduces several advantages into SiGe HBTs, including, (a) an increase in the collector current at the same base-emitter value, and thus a higher current gain and a lower power dissipation, (b) a decrease in the output resistance, (c) an increase in the cutoff frequency f_T, and (d) an increase in the maximum oscillation frequency f_{max}. The last one is mainly the consequence of the decrease of the base resistance $r_b b$ without a significant degradation

in the current gain. SiGe has lower diffusion coefficient for boron than Si does, and thus provides such possibility. The current SiGe:C technique improves the performance even more.

1.2 Extreme Environment Applications

In addition to its growing importance in emerging integrated circuits needed for RF through mm-wave communications systems, SiGe HBTs are also being pursued for a host of so-called "extreme environment" applications [6]. Such applications involve, for instance, operation under radiation exposure (e.g., for space exploration or Earth orbit) [7], [8], as well as at reduced (cryogenic) temperatures (e.g., to 77 K or even 4 K – e.g., the surface of the Moon can reach 43 K in the shadowed polar craters) [9]-[12].

SiGe technology is a natural fit for such niche applications because it possesses inherent ionizing radiation tolerance as fabricated, and the impact of bandgap engineering on the speed of SiGe HBTs is generally favorably affected by cooling, as evidenced by the recent report of record 510 GHz peak f_T prototype 4^{th}-generation SiGe HBT operating at 4.5 K [13]. Though Si BJTs are known to have performance degradation at reduced temperatures because of heavy doping and carrier freezeout, SiGe HBTs can offset these negative impact by increasing base doping level. More imporatantly, all the key parameters of SiGe HBTs are thermally-activated functions of the amount of bandgap reduction in the base, and a small amount of Ge is already sufficient to attain the improved cryogenic performance even without any special low-temperature optimization for the devices.

Clearly, however, detailed understanding of the subtleties of device operation under these extreme operational conditions is required if circuit applications are to follow. Unusual phenomena can indeed be found in SiGe HBTs, especially at very low temperatures. Trap-assisted tunneling, for example, induces a minority carrier transport mechanism that can produce a non-ideal collector current component at temperatures below 77 K [12].

In addition, an I-V hysteresis and negative differential resistance (NDR) was recently observed in the forced-I_B output characteristics of aggressively-scaled 4^{th}-generation SiGe HBTs, and was shown to be the result of enhanced tunneling and recombination at high injection at cryogenic temperatures [14].

1.3 High Injection and Low-Temperature

As a band edge phenomenon, heterojunction barrier effect (HBE) becomes increasingly important in SiGe HBTs as the operating temperature decreases, due to its thermally-activated nature. HBE was first observed in GaAs/GaAlAs HBTs [16], [17]. Theory predicting the high-injection HBE in SiGe HBTs was presented in [18] and the effect was later investigated in the measurement of SiGe HBTs operating at low temperatures and shown to strongly impact both *dc* and *ac* device behavior [19]. Subsequent research focused on the optimization of SiGe HBTs in the presence of HBE [20] (across temperature) and improved compact modeling for circuit design [21]. These investigations were conducted at temperatures above 77 K, however, and thus HBE were not assessed at very deep cryogenic temperatures approaching, for example, liquid helium (4.2 K). The impact of SiGe HBT technology scaling on HBE as a function of temperature has also not to-date been carefully addressed, and is particularly relevant in HBE, since collector doping and Ge concentration and profile shape are well-known to play a strong role.

1.4 Researches on Negative Differential Resistance

Research on negative differential resistance (NDR) dates to the advent of semiconductor devices, when different mechanisms of NDR and their applications were studied extensively. Three mechanisms are primarily responsible for NDR in semiconductors, including: field-excited transfer of electrons from a low-mass valley to a high-mass valley of the conduction band [22]-[24], field-induced capture of electrons [25], [26], and Fowler-Nordheim

tunneling of electrons in wide-gap materials [27]. These negative resistance effects, however, are intrinsic properties of the related III-V materials, and thus are irrelevant to the group-IV semiconductors (e.g., Si and Ge).

Meanwhile, semiconductor tunnel structures which exhibit NDR can be found in both III-V and group-IV devices, and examples include Esaki diodes [28], double-barrier resonant tunneling diodes [29], single-barrier tunneling diodes [30], [31], and resonant interband tunneling devices [32]. The integration of resonant tunneling devices into commercially-available IC processing (e.g., in Si) has been recently pursued for mixed-signal and fast digital (logic/memory) applications [33]-[40]. Other Si-based NDR transistors include such devices as bistable gated bipolar transistor that is of potential interest to digital circuits [41], [42]. Compared to all such NDR devices, the NDR effects described in the present work has fundamentally different physical origin.

In this thesis work, we present the first comprehensive investigation of a new HBE-induced NDR effect and collector-current kink effect in SiGe HBTs operated down to temperatures as low as 5.4 K [15]. Following a presentation of the measured results highlighting the observed effects in Chapter II, Chapter III proposes a physical mechanism to explain these observations, followed in Chapter IV by TCAD simulations supporting our claims. The impact of doping and Ge profile on the observed effects, as well as the scaling implications are addressed in Chapter V, followed by a discussion of the *ac* consequences. Finally, a comparison of two fundamentally different NDR phenomena in SiGe HBTs operating at deep cryogenic temperatures is presented, including circuit-relevant design implications involving the impact of forced-current *vs.* forced-voltage input drive, followed by a summary.

1.5 Measurement Setup

The cryogenic device measurements were made using an on-wafer, open-cycle, liquid helium cryogenic probe system capable of *dc* to 35 GHz operation from 350 K to 5 K. The

system thermometry was calibrated by comparing device characteristics inside the system with those measured directly immersed in both liquid nitrogen (77.3 K). The temperature accuracy is believed to be better than 1 K, and is stable at intermediate temperatures. The chuck temperature was independently verified to be 4.5 K (liquid helium = 4.2 K), although we believe the actual device temperature is at least several K above this temperature due to the inherent thermal loading of the probes when in contact with the wafer. For consistency the chuck temperature is specified in our data. The measured data are repeatable and have been exhaustively verified using a variety of techniques.

An Agilent 4156 Semiconductor Parameter Analyser was used for *dc* device characterization, and an Agilent 8510C Vector Network Analyzer was used for *ac* measurements. Standard calibration and de-embedding techniques were used at each measurement temperature.

Table 1: Comparison of Key Performance Parameters for SiGe Technologies from IBM.

Parameters	5HP	6HP	7HP	8HP	9T
Lithographic node (μm)	0.5	0.25	0.18	0.13	0.13
f_T (GHz)	47	47	120	210	300
f_{max} (GHz)	65	65	100	285	350
β	100	100	350	300	650
BV_{CEO} (V)	3.4	3.4	1.8	1.7	1.7
BV_{CBO} (V)	10.5	10.5	6.5	5.5	5.6
J_C @ peak f_T (mA/μm^2)	1.5	1.5	8	12	19

CHAPTER 2

THE NOVEL EFFECTS

Unless specifically indicated, all data presented in this paper are from the commercially-available IBM 5AM SiGe HBT BiCMOS technology, which features 50 GHz peak f_T SiGe HBTs at 300 K [45]. The technology details of the 3^{rd}-generation (200 GHz peak f_T at 300 K)and 4^{th}-generation (350 GHz peak f_T at 300 K) SiGe HBTs also discussed in this paper can be found in [46] and [47], respectively.

2.1 Test Structure Designs

The IBM 5AM SiGe HBT test structures for *ac* and *dc* measurements were specially designed for NASA ETDP phase I project, and was later optimized during phase II. The BiCMOS technology has four layers of metal that are functioning properly over the temperature range required. A full view of all the *dc* test structures is demonstrated in Fig. 1, where 14 columns of transistors with three devices in each columns are shown. In Fig. 2, a standard 0.5×2.5 μm^2 SiGe HBT is laid down with a substrate contact right beside it. The substrate contact is used to minimize the parasitic resistance to the substrate for better modeling.

The *ac* test structures are carefully designed to exclude impact from parasitics as much as possible. Fig. 3 gives the full view of all the 17 *ac* test structures, where standard OPEN/SHORT/THROUGH structures are used for de-embedding. The test structure design of a standard 0.5×2.5 μm^2 SiGe HBT is shown in parallel with the corresponding OPEN/SHORT/THROUGH structures (Fig. 5). The substrate contact is also used here to minimize the parasitic resistance to the substrate. In addition, all thin lines of metal

were avoided during the entire design to eliminate any petential influence of parasitic inductances. The use of the bottom three metal layers were minimized to decrease parasitic capacitances and resistances, as the top layer is farthest away from the active region of the device and is the thickest of all the four metal layers. Diva LVS was run to verify the design (Fig. 4).

The design of the *ac* test structures for larger 0.5×20×2 SiGe HBTs requires wider metal path to sustain the larger current flows (Fig. 6). Tradeoff exists, as the consequent bigger area of metal usually means larger parasitic capacitances, which may especially have certain impact on the final f_{max} extraction. One needs to be very careful in finding the balance point in this tradeoff.

2.2 Negative Differential Resistance

A new device effect, a negative differential resistance (NDR) region in the forced-V_{BE} output characteristics, is consistently observed of these 1^{st}-generation SiGe HBTs operating at high-injection at deep cryogenic temperatures (Fig. 7). A control Si BJT (with nearly the same doping profile but without Ge) was also measured and no NDR is observed in Fig. 7, indicating that this NDR effect is clearly Ge-induced.

The excess collector current ($\triangle I_C$) of the SiGe HBT is defined as the collector current (I_C) difference directly before and after the observed NDR occurs, or,

$$\triangle I_C = I_{C,peak} - I_{C,valley}, \tag{1}$$

where $I_{C,peak}$ (the peak current) is the maximum collector current immediately before the NDR, and $I_{C,valley}$ (the valley current) is the minimum collector current immediately after the NDR . The $\triangle I_C$ is proportional to $I_{C,peak}$ to the first order (Fig. 9). To quantitatively assess the temperature dependence of the NDR, an excess current ratio (ECR) is defined

as the average of all the measured $\triangle I_C$ normalized by $I_{C,peak}$, or,

$$ECR = Avg\left(\frac{\triangle I_C}{I_{C,peak}}\right) = Avg\left(\frac{I_{C,peak} - I_{C,valley}}{I_{C,peak}}\right) = Avg\left(1 - \frac{I_{C,valley}}{I_{C,peak}}\right), \quad (2)$$

where $Avg()$ means the mathematical average value.

In the literature, peak-to-valley current ratio ($PVCR$) is more often used as a figure-of-merit for NDR devices, and is usually defined as,

$$PVCR = \frac{I_{C,peak}}{I_{C,valley}}, \quad (3)$$

For convenience and better insight, ECR is used in the present paper, but can be easily converted to $PVCR$ using,

$$ECR = Avg\left(1 - \frac{1}{PVCR}\right), \quad (4)$$

The extracted ECR linearly increases as temperature (T) decreases from 93 K to 5.4 K, as shown in the inset of Fig. 9. The NDR is almost negligible at 93 K, and disappears entirely at $T > 93$K. The ECR as a function of T can be quantitatively expressed as,

$$ECR(T) = a \cdot T + b, \quad (5)$$

with fitting parameters $a = -0.00367\ K^{-1}$ and $b = 0.38282$. Equation (5) can be used to predict the magnitude of NDR for any given collector-current level at any temperature for this SiGe technology, and can be similarly applied to any SiGe process technology as a design aid. For reference, the resultant $PVCR$ is 1.3 at 43K and rises to 1.6 at 5.4K. These are reasonable values for NDR, given that similar $PVCR$ numbers are reported in resonant tunneling diodes (Table 2).

2.3 Collector-Current Kink Effect

An anomalous collector current kink is also observed in the Gummel characteristics of the SiGe HBT at temperatures below about 100 K (Fig. 10). The I_C kink effect is characterized

by a sharp I_C increase at a given V_{BE}, resulting in a large "spike" in the transconductance (g_m), as shown in the dotted curve in Fig. 11).

From a careful examination of the T-dependent Gummel characteristics in Fig. 10, the I_C kink can be seen to be clearly associated with the onset of classical HBE, since the I_C kink occurs at the identical V_{BE} as the sharp I_B increase produced by HBE. However, the observed I_C increase is fundamentally different from the impact of conventional HBE on the device, where I_C is clamped (decreases) because of the induced conduction band barrier at the SiGe-Si base-collector heterojunction [19], [21]. Note that conventional HBE theory predicts a resultant decrease, not an increase, in I_C under these conditions, and thus is clearly different from what have been previously reported in the context of HBE.

Neither the I_C kink nor the resultant g_m spike can be found in the control Si BJT at 43 K (Fig. 16), again highlighting the Ge-dependence of this unique effect. In addition, measurements of the emitter-base diode of the SiGe HBT over temperature, while leaving collector terminal open, shows no such kink effect in the diode current, which further demonstrates that the effect is not associated with the emitter-base (EB) junction.

In fact, the NDR observed in the forced-V_{BE} output characteristics, and the I_C kink in the Gummel characteristics, are produced by the same physical mechanism. Fig. 11 shows the Gummel characteristics at different V_{CB}'s on a linear scale, and indicates that a smaller V_{CB} results in a suddenly (and unexpectedly) higher I_C at certain bias points (e.g., points A and B in Figs. 7 and 11), since the sudden increase in I_C occurs at smaller V_{BE} for lower V_{CB}. This produces an NDR region in the forced-V_{BE} output characteristics, where higher V_{CE} produces a lower I_C, as illustrated explicitly in Fig. 7.

Finally, any possibility of device oscillation during measurement as a physical origin of the observed NDR has been systematically eliminated. The fact that a control Si BJT does not show these novel NDR effects is important in this context, because the Si BJT is identical to the SiGe HBT in every way including the device and pad layout, and used

an identical measurement setup. Various additional techniques were used to ensure the robustness of the data. First, measurements were repeated on several different experimental setups, including: 1) an on-wafer cryogenic probe station with measurements using co-linear *dc* probes that are designed specifically for low temperature measurements; 2) an on-wafer cryogenic probe station with measurements using G-S-G shielded probes on different *ac* test structures; and 3) a closed-cycle helium cryostat system using 28-pin DIP packages and wire-bonded samples. These three distinct setups produce consistent and repeatable results. Second, test structures with different device layouts were measured. Besides the standard test structures provided by IBM, different *ac* and *dc* test structures are also designed and measured, and all show identical results. Third, devices of different geometries were measured. Large-sized HBTs are known to be generally more immune to oscillations because of the smaller impact of layout parasitics. In addition to the standard 0.5×2.5 and 0.5×1.0 μm^2 SiGe HBTs, we also measured the 0.5×20×2 μm^2 power transistor. All of these devices show the same novel NDR effects. Fourth, different measurement techniques were used in the 4155 Semiconductor Parameter Analyzer in order to verify that the data are robust. For instance, sweeping V_{BE} in both directions produces exactly the same Gummel characteristics, and sweeping V_{CE} in both directions produces identical output characteristics. "Long" vs. "short" integration times on the 4155 was also chosen for the NDR and I_C kink effect regions of the curves, showing no differences. Measuring a single bias point over a certain period of time was also adopted in the NDR and IC kink effect regions, and produced stable and reproducible results. In summary, we have taken great pains to ensure that the reported data are robust, and we have high confidence that the observed effects are in fact real.

Table 2: Comparison of $PVCR$ in SiGe HBTs and in different Si resonant tunneling diodes

Reference	Device	PVCR	Temperature (K)
This work	SiGe HBT	1.3	43
		1.6	5.4
[43]	Si/SiGe double barrier diodes	1.2	room-T
		1.5	77
[33]	Si/SiGe RTD	2.9	room-T
[44]	Si Esaki diode	1.12 - 1.08	4.2 - 325

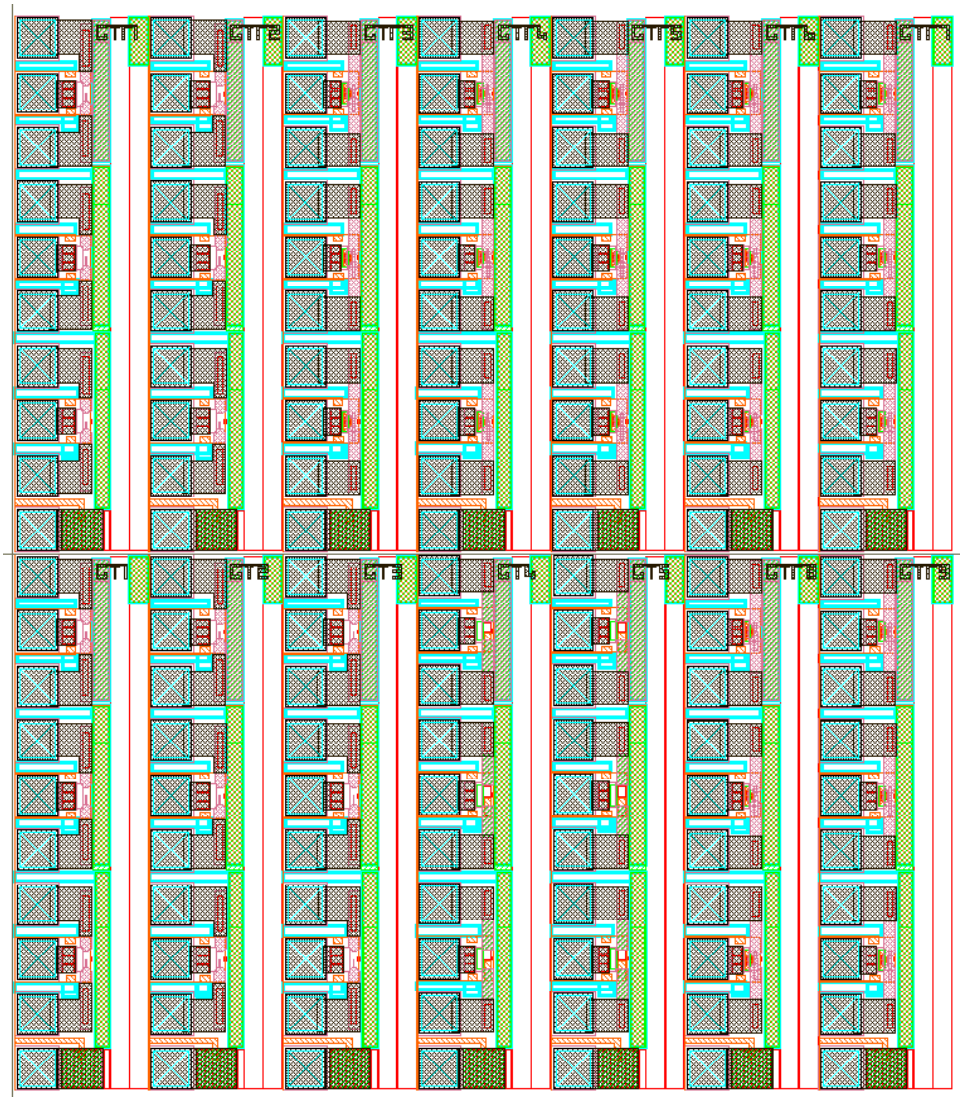

Figure 1: Test structure designs for *dc* measurement of SiGe HBTs.

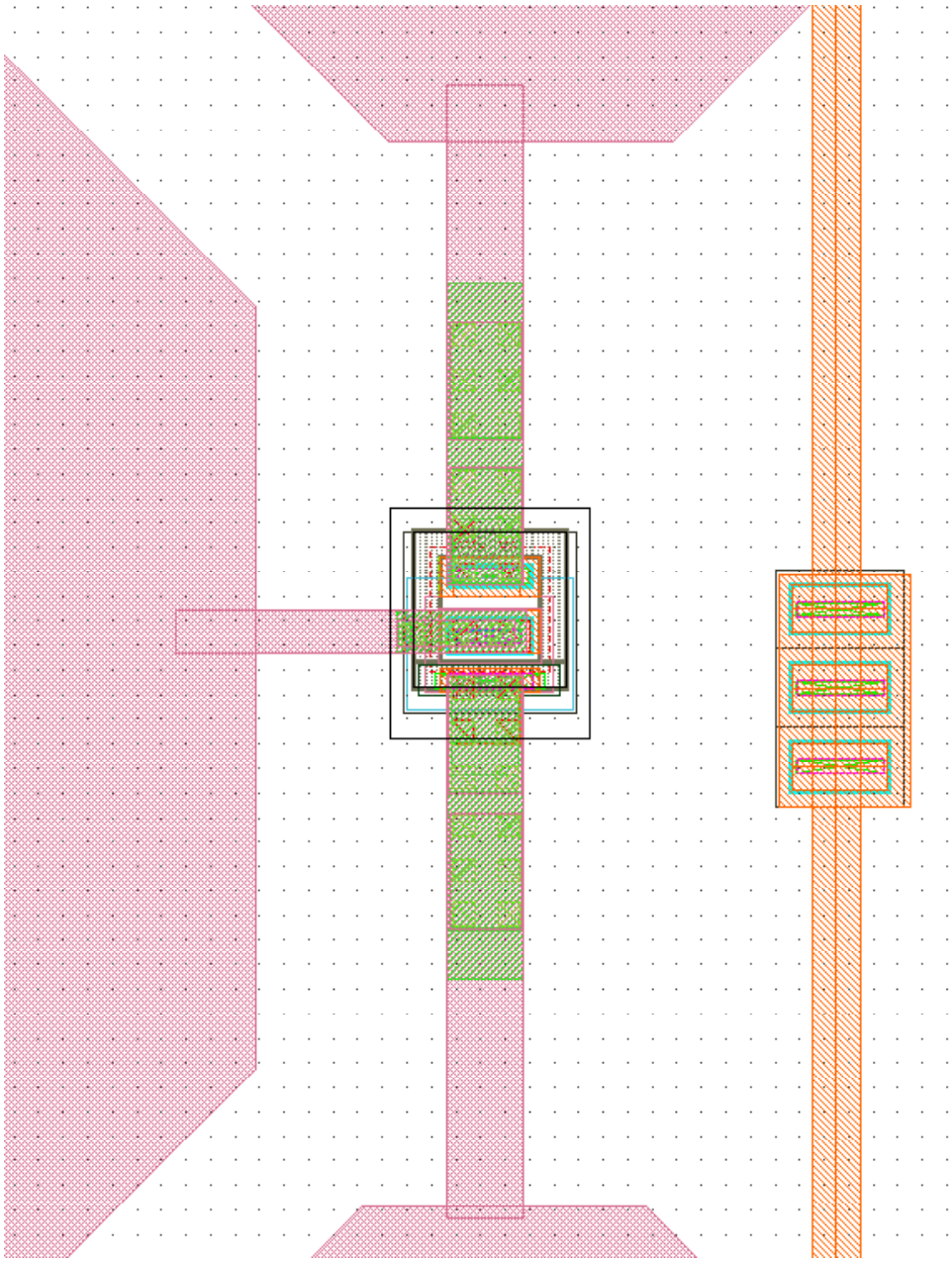

Figure 2: *dc* test structure for a single SiGe HBT.

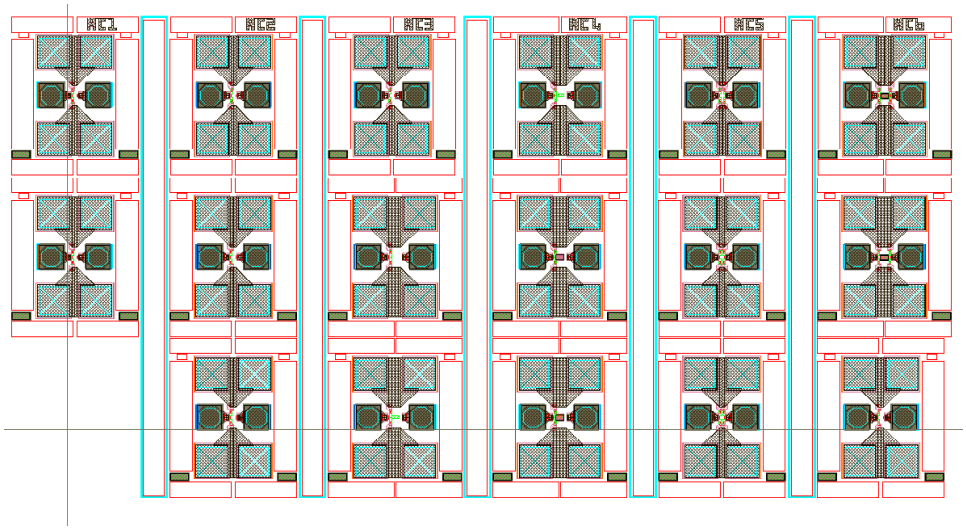

Figure 3: Test structure designs for *ac* measurement of SiGe HBTs.

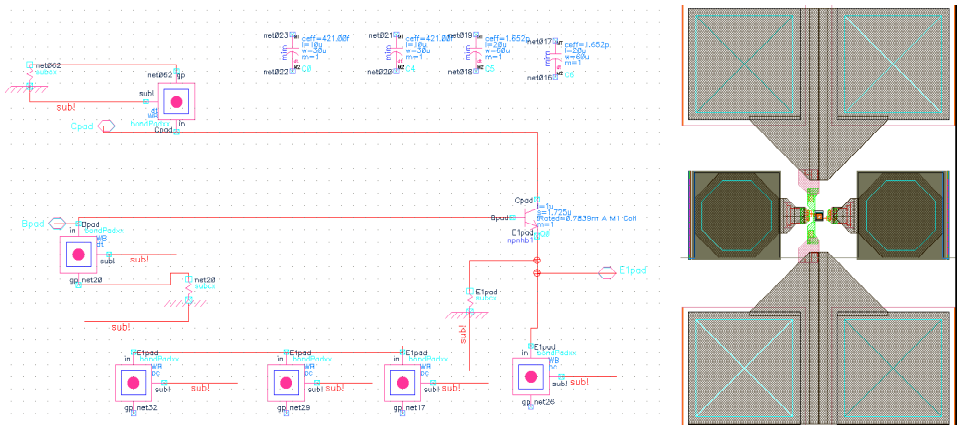

Figure 4: *ac* test structure for a SiGe HBT (a) layout versus (b) schematics.

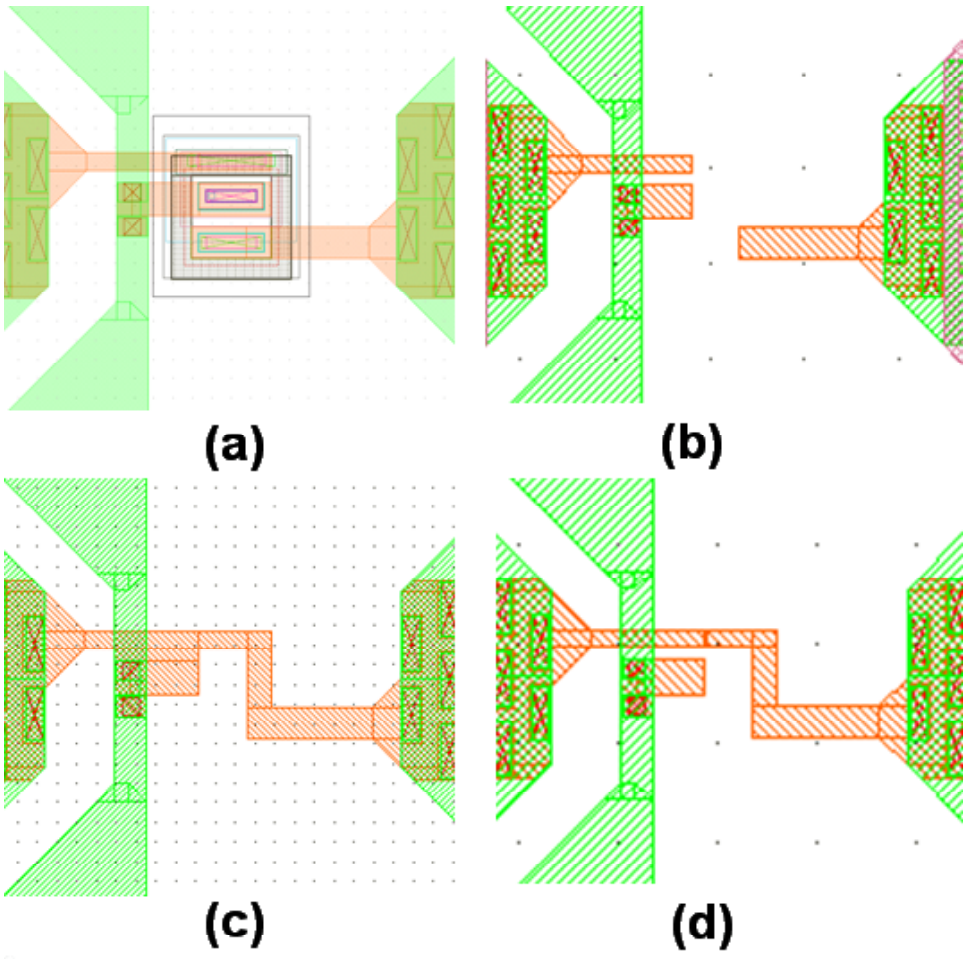

Figure 5: Layout for ac test structures of a (a) single standard-sized SiGe HBT (b) open (c) short and (d) through structures.

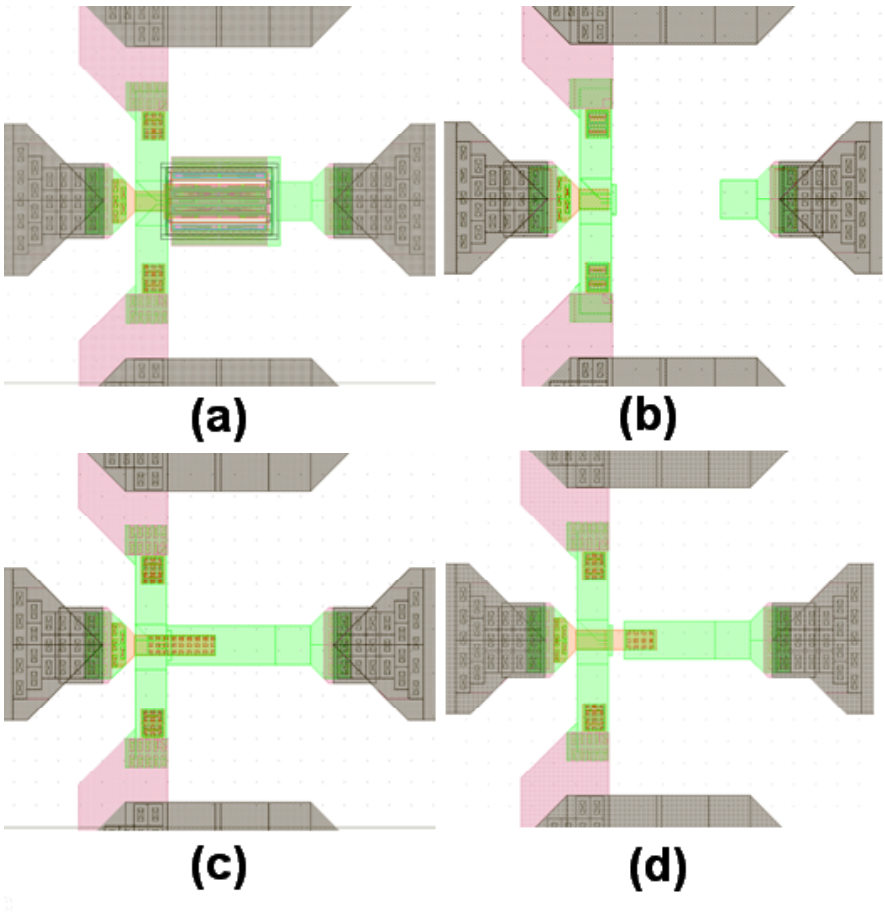

Figure 6: Layout for ac test structures of a (a) single big-sized SiGe HBT (b) open (c) short and (d) through structures.

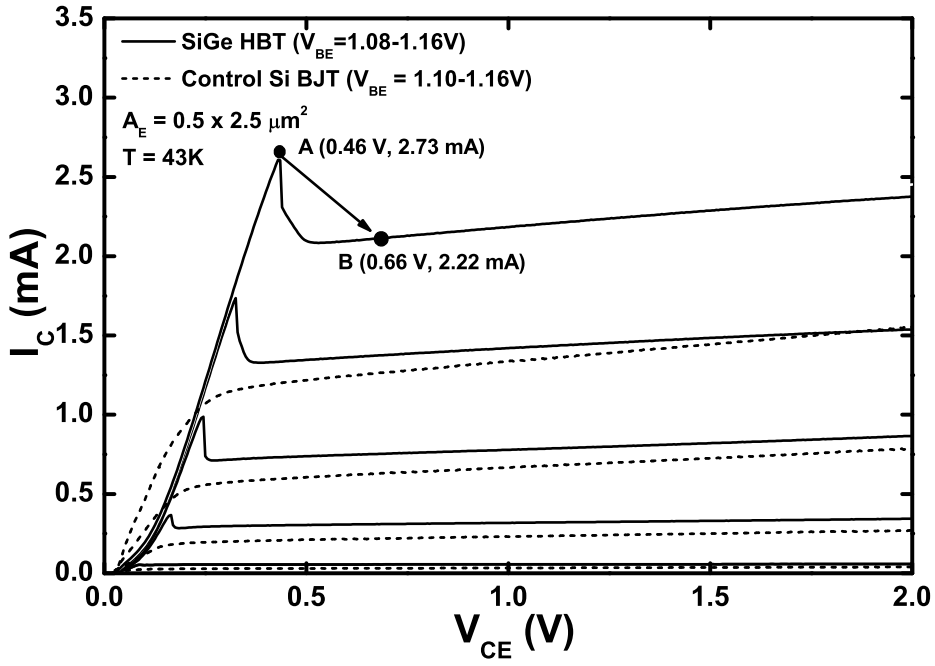

Figure 7: Comparison of the measured forced-V_{BE} output characteristics of SiGe HBT and the control Si BJT at 43K.

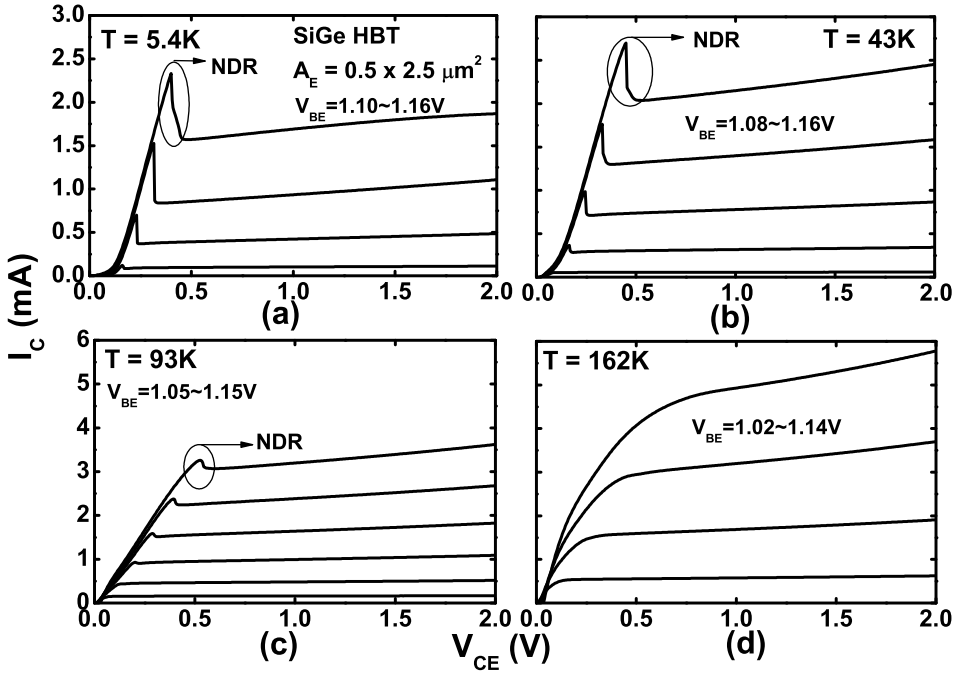

Figure 8: Measured forced-V_{BE} output characteristics of a SiGe HBT at (a)5.4K, (b) 43K, (c) 93K, and (d) 162K. NDR is observed in (a) - (c).

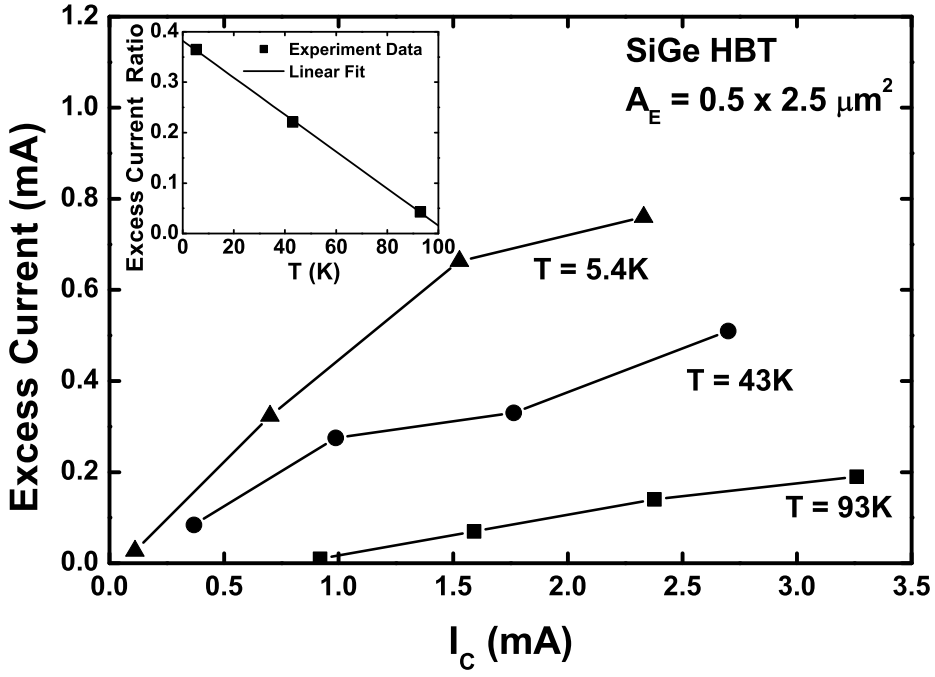

Figure 9: The excess current for NDR (defined as the I_C difference before and after the NDR occurs) in the forced-V_{BE} output characteristics *vs.* collector current at 5.4K, 43K and 93K. Inset shows the linear fit for the excess current ratio (defined as the excess current divided by I_C before the NDR) across temperatures.

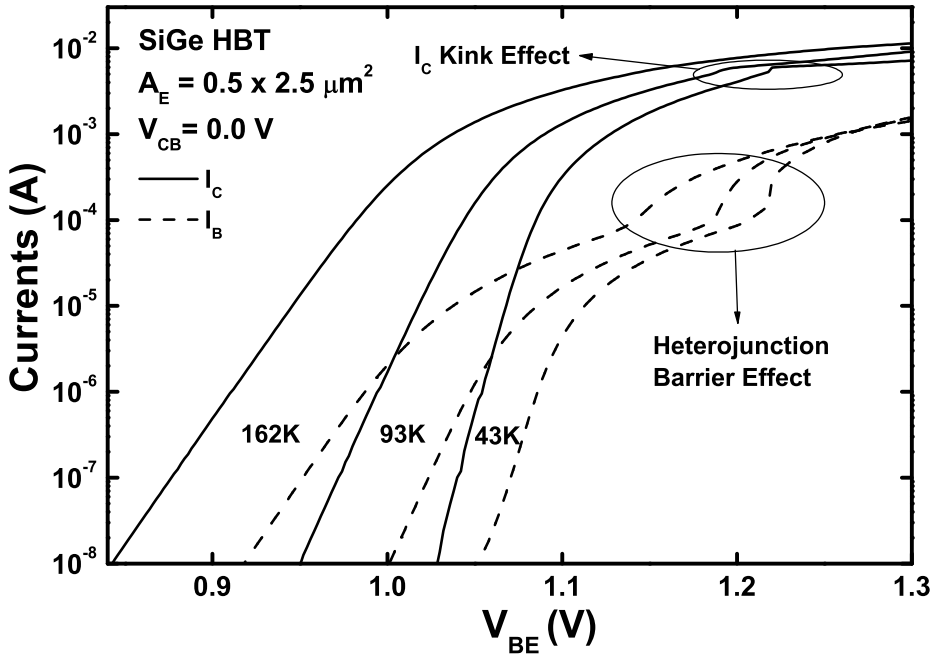

Figure 10: Measured Gummel characteristics of the SiGe HBT at 43K, 93K, and 162K. The I_C kink effect can be observed at 93K and below, together with the sudden I_B increase representing the onset of heterojunction barrier effect (HBE).

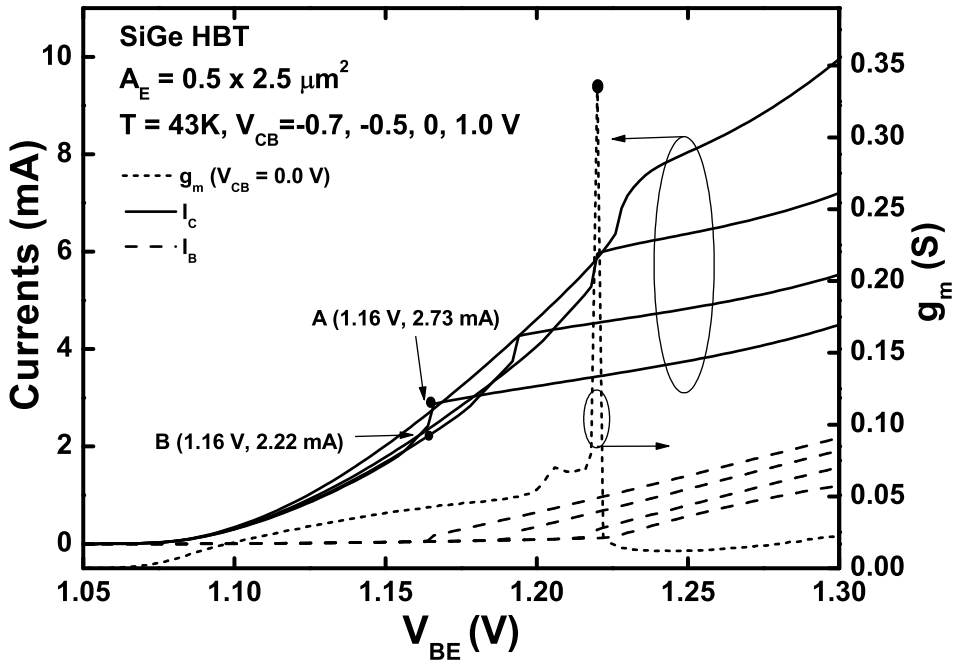

Figure 11: Measured Gummel characteristics (with currents on a linear scale) of the SiGe HBT at 43K and at different V_{CB}'s. Also shown is the transistor transconductance (g_m) at V_{CB}=0V. Points A and B corresponds to points A and B in Figure 7, indicating the intrinsic relationship between NDR and the kink effect.

CHAPTER 3

PHYSICAL MECHANISM

The measurement results in the previous chapter strongly suggest a direct connection between the observed NDR and I_C kink with classical HBE. However, since conventional HBE theory in HBTs predicts only an I_C decrease and a sudden increase in I_B at a V_{BE} (J_C) sufficient to turn-on HBE for any fixed V_{CB} [21], we must revisit the physical origins of HBE, and explicitly examine how device operation at deep cryogenic temperatures can change the coupling of HBE to the transistor response.

3.1 A Brief Review of HBE

In homojunction bipolar transistors, high-injection performance is mainly limited by Kirk effect [48] and Webster-Rittner effect [49], [50]. In heterojunction bipolar transistors operating at high injection, however, the combination of Kirk effect and HBE limit device performance. Physically, in HBE, when J_C gets sufficiently large, the increased minority carrier concentration in the CB space charge region acts to compensate the local ionized donors, causing the original CB electric field to collapse. Classical Kirk effect pushes the boundary of the CB space charge region further into the selectively implanted collector (SIC) region, gradually exposing the Si/SiGe heterojunction interface that was originally masked by the band bending in the CB space charge region. The exposure of the valence band barrier induces a conduction band barrier that blocks the hole injection into SIC needed to maintain charge neutrality, producing a pile-up of holes at the hetero-interface. This local hole accumulation in-turn leads to a conduction band barrier that opposes electron transport from the base to the collector, rapidly degrading both *dc* and *ac* device performance.

Based on the quantitative theory of *Liang et al.* [21], the deviation of charge in the base ($\triangle Q_b$) as a function of J_C due to the barrier effect can be expressed as follows,

$$\triangle Q\left(J_C\right) = C \cdot J_{C,barrier} \cdot \left(e^{\triangle E_{C,barrier}/2kT}\right) \cdot \left[\frac{J_C}{J_{C,barrier}} - ln\left(\frac{J_C}{J_{C,barrier}}\right) - 1\right] \tag{6}$$

where C is a (constant) fitting parameter, $\triangle E_{C,barrier}$ is the height of the conduction band barrier, and $J_{C,barrier}$ is the critical onset current density for barrier effect. Note that $J_{C,barrier}$ is a monotonically increasing function of V_{CB}, since $\triangle E_{C,barrier}$ gradually decreases as V_{CB} increases. This is because the conduction band edge (E_C) is effectively "pulled down" by the higher V_{CB} imposed on the space charge region of the CB junction via Poisson's equation and the continuity equations.

Consequently, this extra base charge storage induces not only a rapid current gain (β) roll-off (degradation) but also a sudden decrease in f_T and f_{max} [51]. More fundamentally, the high-injection base transport under classical HBE differs from that of Si BJT in the following ways: the electron diffusion current component decreases (sometimes even to negative value) due to a reduction in the electron density gradient in the base, as shown in Fig. 12, and the drift current component now dominates I_C because of the large carrier density. In addition, the extra HBE-induced accumulated electron/hole charges act as a local dipole, imposing an inverse electric field that acts to weaken the drift current in this region. I_C is thus strongly reduced under HBE, while I_B rises rapidly due to enhanced recombination, strongly degrading the current gain and f_T of the device.

3.2 Enhanced Positive Feedback in HBE at Deep Cryogenic Temperatures

HBE at deep cryogenic temperatures is more complicated. The impact of the heterojunction barrier on the charge accumulation is generally larger at very low temperatures because HBE is a thermally-activated band-edge phenomenon, leading to much higher electron concentrations in the base at low temperatures than at higher temperatures (at say fixed J_C). A comparison of the simulated conduction band edge (E_C) and electron density (n)

are given in Fig. 12, where about 10 times more HBE-induced electrons are accumulated in the base at 77 K than at 300 K at a similar current density. In the base region of the SiGe HBT, the electron current density J_n can be expressed as,

$$\vec{J}_n = q \cdot \mu_n \cdot \nabla \left(\frac{n \cdot k \cdot T}{q} \right) + q \cdot n \cdot \mu_n \cdot \vec{E} \tag{7}$$

where the first term of $\vec{J}_n$ represents the diffusion component of the total electron current density, and the second term is the drift current component [52]. Therefore, significantly larger drift current component is expected at cryogenic temperatures.

With the increase of the collector current density at higher temperatures, the inverse electric field caused by the conduction band barrier and Kirk effect mutually opposes the further increase of the electrons flowing from emitter to collector; consequently the barrier height, the electron concentration, and the electron current density form a negative feedback loop that acts to "stablize" the total collector current. At deep cryogenic temperatures, however, the stronger HBE-induced electron concentration in the base adds up to the total drift current overcoming the negative influence of the inverse field on J_C, which in turn greatly enhances the heterojunction barrier as well as its impact on the collector current density. As a result, the barrier height, the electron concentration, and the electron current density act to produce a positive feedback loop at the onset of HBE. This greatly accelerates the formation of the heterojunction barrier, yielding a much more rapid electron accumulation at the onset of the HBE, which not only decreases the diffusion current component, but also enhances the drift current component at a much higher rate, eventually producing a sudden I_C increase in the Gummel plot for a fixed V_{CB}. The transformation of the negative feedback at higher temperatures into the positive feedback at deep cryogenic temperatures is illustrated in Fig. 13 (a) and (b). This induced positive feedback loop gets increasingly stronger (enhanced) as the temperature further drops.

The observed NDR behavior in these SiGe HBTs is a direct consequence of the above process. During the forced-V_{BE} measurement, the conduction band barrier gradually decreases as V_{CE} (and thus V_{CB}) increases, because (E_C) is effectively "pulled down" by the

higher V_{CB} imposed on the space charge region of the CB junction. As a result, the number of the accumulated electrons in the base region decreases. The barrier height is more sensitive to V_{CB} at lower temperatures also due to the enhanced positive feedback between the barrier height, the charge accumulation, and the current density with cooling, as shown in Fig. 13(b). This causes a more rapid decrease of n when the HBE is turned off by increasing V_{CE} at low temperature, giving rise to an NDR in the output characteristics.

In addition, cooling effectively turns-on HBE at a higher J_C than at 300 K due to the shift in the built-in potential of the CB junction [51], together with the slight increase in the electron saturation velocity at low temperature [9]. These effects further contribute to the total enhancement of the positive feedback of the loop depicted in Fig. 13(b) at cryogenic temperatures, effectively magnifying the phenomena.

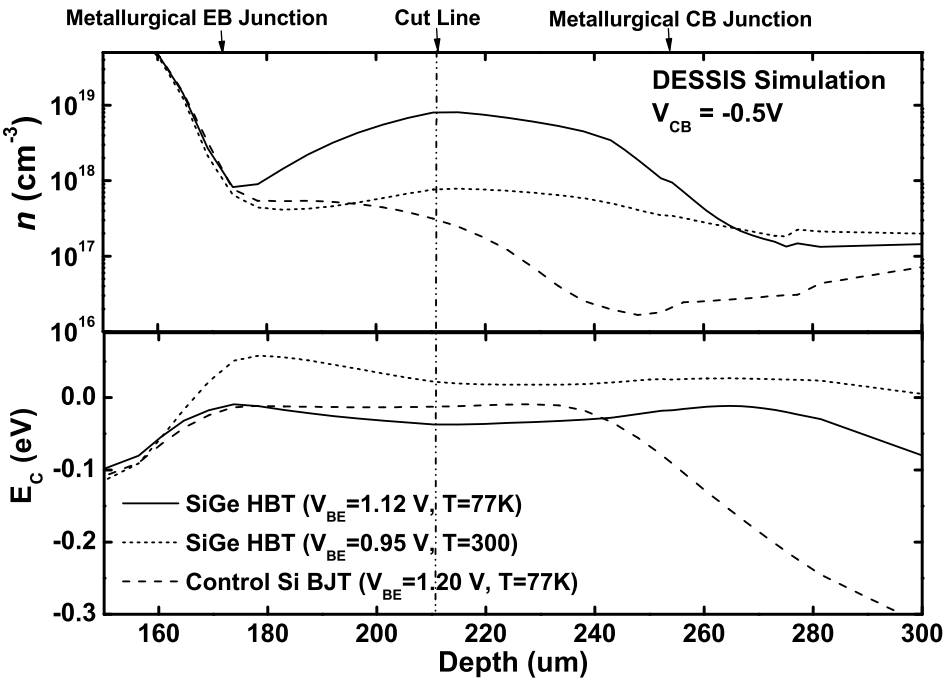

Figure 12: Simulated conduction band edge (E_C) and electron density (n) as functions of depth for the SiGe HBT at 77K, at 300K and the control Si BJT at 77K. The V_{BE}'s are chosen to ensure comparable collector current for all the three situations. Positions for the metallurgical junctions and the cut line are marked.

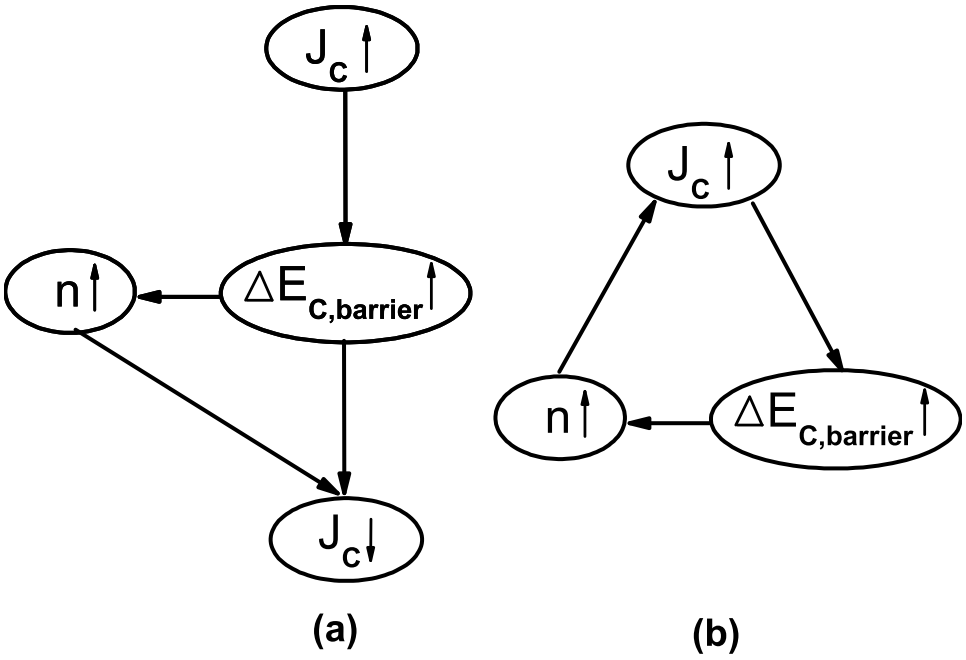

Figure 13: The feedback loop of the key physical parameters happening at heterojunction barrier effect and at (a) higher temperatures forming a negative feedback, (b) deep cryogenic temperatures forming a positive feedback.

CHAPTER 4

SIMULATION RESULTS

Both the NDR and the I_C kink effect can be qualitatively captured using 2-D DESSIS simulations. The 2-D doping and Ge profiles and device mesh were based on SIMS data and the actual transistor layout dimensions. The simulation parameters have been carefully calibrated to fit the measured *dc* and *ac* characteristics of the transistor across temperature. 77 K was the lowest simulation temperature used because robust convergence at high-injection could not be easily attained below this temperature.

Fig. 14 shows the simulation results of the SiGe HBT at 77 K, clearly showing the NDR, the I_C kink effect, and the g_m spike. No such effects are found in the simulations of the control Si BJT at 77 K or the SiGe HBT operating at 300 K (Fig. 15). Turning off the hydrodynamic model in DESSIS makes little difference in the result, which indicates that the NDR effects can be explained within the traditional drift-diffusion framework (turning off carrier freeze-out in the simulation produces the same trends, also showing that carrier freeze-out also does not play a strong role).

4.1 Collector-current kink effect

The barrier height and n in the base at the onset of HBE as functions of V_{BE} are shown in Fig. 17 and 18. The snapshot of these two parameters are taken at the position of the cut line indicated in Fig. 12.

The SiGe HBT operating at 300 K shows a gradual increase in the barrier height and the resultant n with increasing V_{BE}; however, both the barrier height and n increase far more rapidly at the onset of HBE in the device operating at 77 K. This is expected in the context of our proposed mechanism, where the positive feedback of the barrier effect is

demonstrated to be greatly enhanced at very low temperatures. Changing the CB bias from 0 V to 1 V helps push the sudden onset of the barrier effect to a higher V_{CB} (from 1.128 V to 1.159 V in this case), as shown in Fig. 17. However, both CB biases at 77 K result in an extremely rapid turn-on of the barrier effect, producing a sudden increase in the barrier height and the drastic increase in charge accumulation, which is clearly different than at room temperature.

The resultant sharp increase in n causes an extra drift current component that adds up to the total collector current, consequently producing the I_C kink and the g_m spike present in the Gummel characteristics of the device. When V_{BE} further increases to the values higher than the kink effect, it takes much more increase in the total current density to induce the same amount of barrier height growth, as the barrier height is eventually limited by bandgap difference between Si and SiGe. Therefore the condition of positive feedback is valid only at the onset of HBE, after which I_C clamps (saturates), as is generally true for HBE.

4.2 The NDR Picture

To shed further light on the mechanism underlying the NDR seen in the forced-V_{BE} output characteristics, two more physical parameters need to be examined in the analysis. Fig. 19-21 provide a comprehensive picture of n, the heterojunction barrier height, the magnitude of the electric field (E), the electron drift current component, and the total electron current component, extracted from a family of points on the forced-V_{BE} characteristics (at both 77 K and 300 K) at the position of the cut line indicated in Fig. 12.

Increasing V_{CE} decreases the base electron accumulation in two ways: a higher V_{CB} changes the Shockley boundary condition and the resultant electron concentration, and in addition, higher V_{CB} decreases the heterojunction barrier height (Fig.19) with a resultant change in carrier concentration (Fig. 20). Consequently, the electron drift current component decreases with increasing V_{CE}, as shown in Fig. 21, even though the electric field increases steadily (Fig. 20). At the same time higher V_{CE} changes the electron gradient and

the resultant electron diffusion current density increases.

These two contributions both affect the total electron current density. At room temperature, when n is smaller and only slightly changes with increasing V_{CE}, the change of the drift current component is expected to be smooth, as shown in the simulated 300 K curve in Fig. 21. Considering the gradually increasing diffusion current component, the total electron current density is a increasing function of V_{CE} (Fig. 21). However, at cryogenic temperatures (e.g., 77 K) there a bias region over which a rapid barrier height decrease occurs because of the enhanced positive feedback in HBE (Fig 19), producing a significant decrease in n (Fig. 20), and a sharp turn-off of the HBE at that bias region. The barrier effect becomes much more sensitive to V_{CB} in this region. The relative decrease in n is more rapid than the increase in E (Fig. 20), and the plot of the resultant drift current density thus shows an unusual sudden drop at 77 K, directly resulting in the fact that the total electron current reaches a peak before decreasing (Fig. 21). This produces the region of NDR in the total I_C, consistent with the measured data.

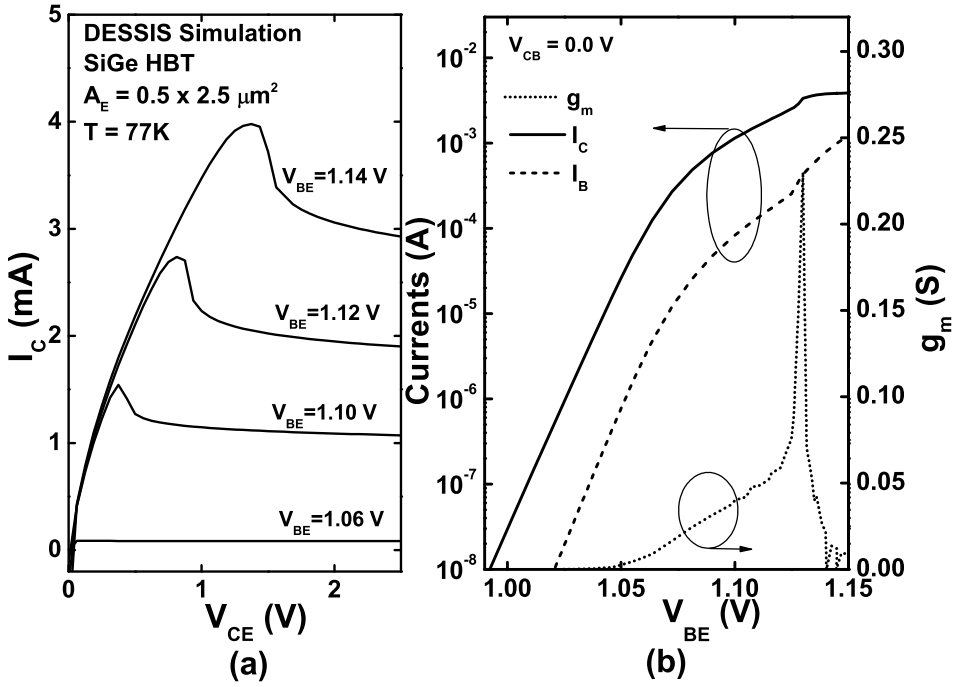

Figure 14: DESSIS simulations of the SiGe HBT at 77K, including (a) forced-V_{BE} output characteristics showing NDR, and (b) Gummel characteristics and the resultant g_m where the I_C kink effect occurs.

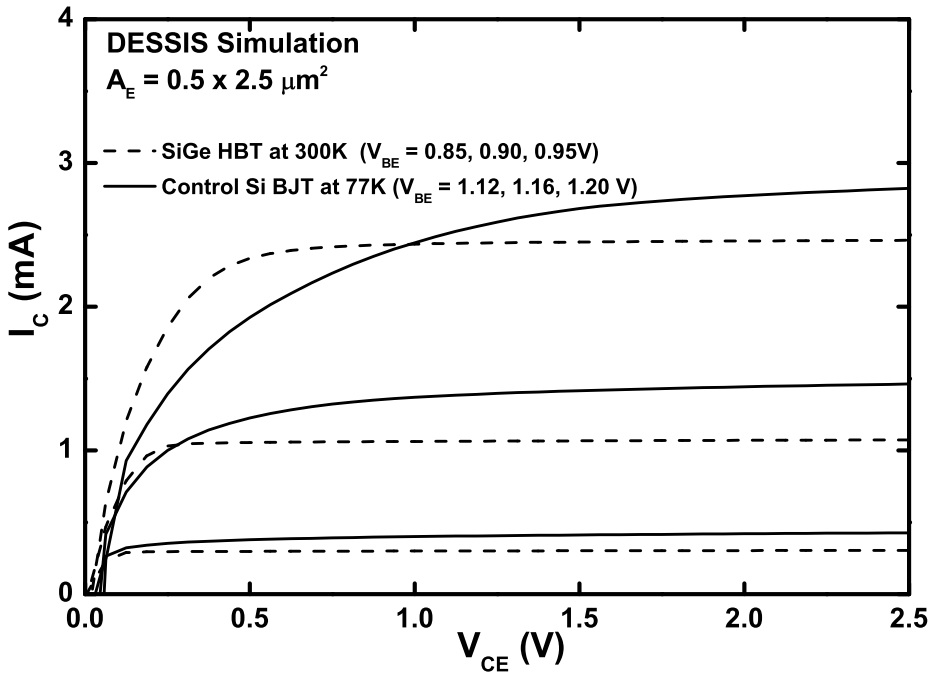

Figure 15: DESSIS simulations of the forced-V_{BE} output characteristics of the SiGe HBT at 300K, and the control Si BJT at 77K.

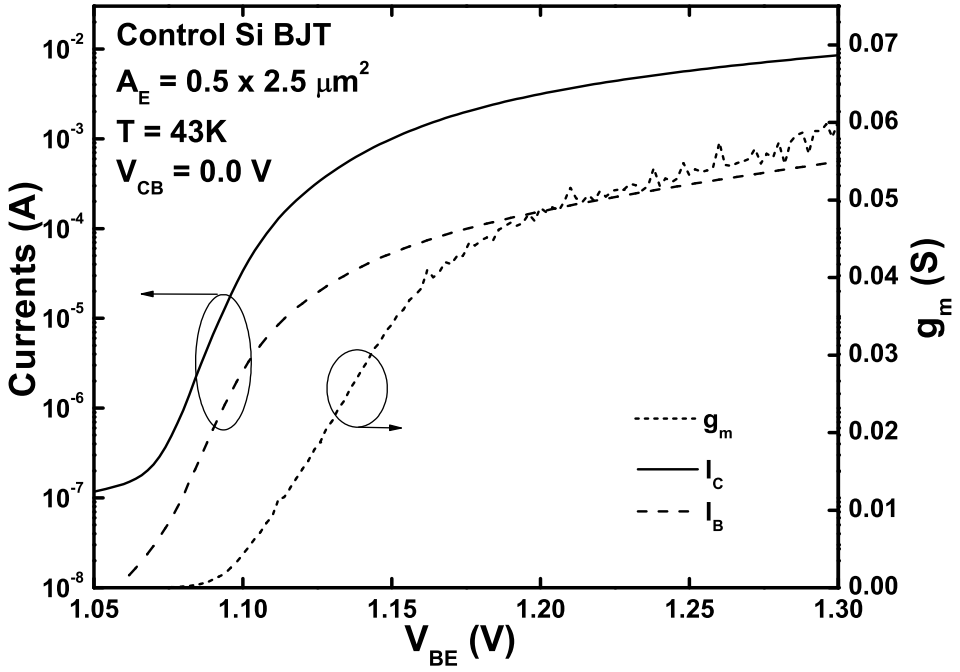

Figure 16: Measured Gummel characteristics of the control Si BJT at 43K and at V_{CB}=0V and V_{CB}=-0.5V. Also shown is the transistor transconductance (g_m) at V_{CB}=0V.

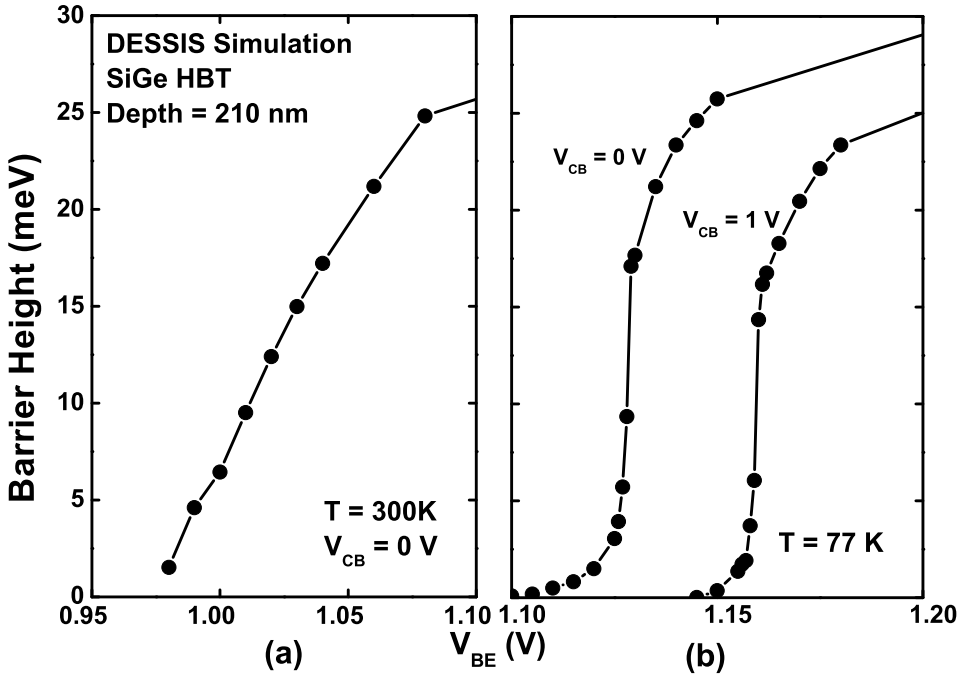

Figure 17: Simulated heterojunction barrier height as functions of V_{CE} for the SiGe HBT at (a) 300K (V_{CB}=0.0 V) and (b) 77K (V_{CB}=0.0 and 1.0 V)

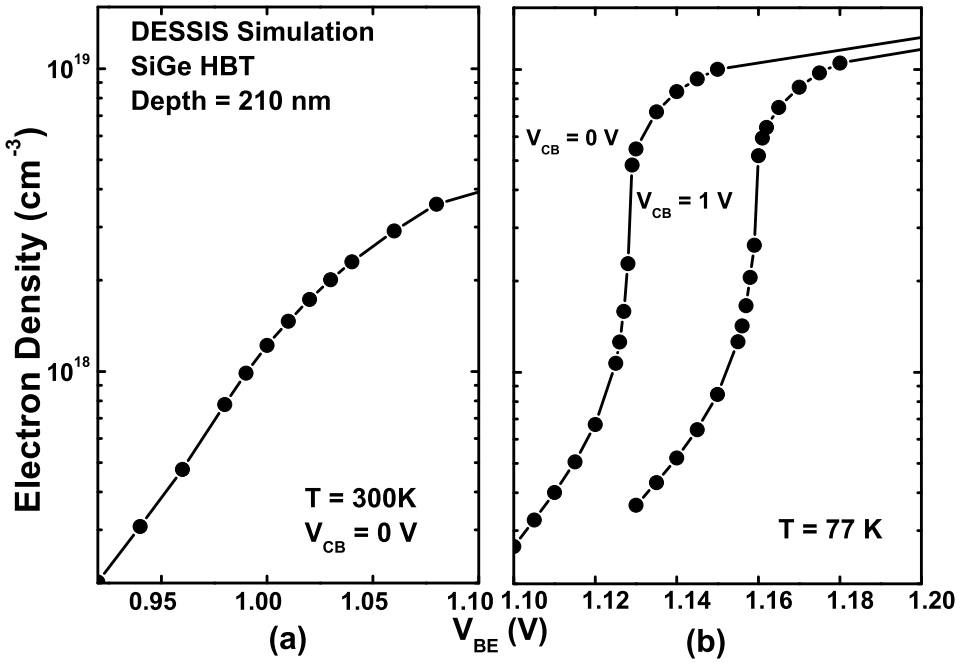

Figure 18: Simulated electron density as a function of V_{BE} for the SiGe HBT at (a) 300K (V_{CB}=0.0 V) and (b) 77K (V_{CB}=0.0 and 1.0 V). The snapshot is taken at the position of the cut line indicated in Figure 12.

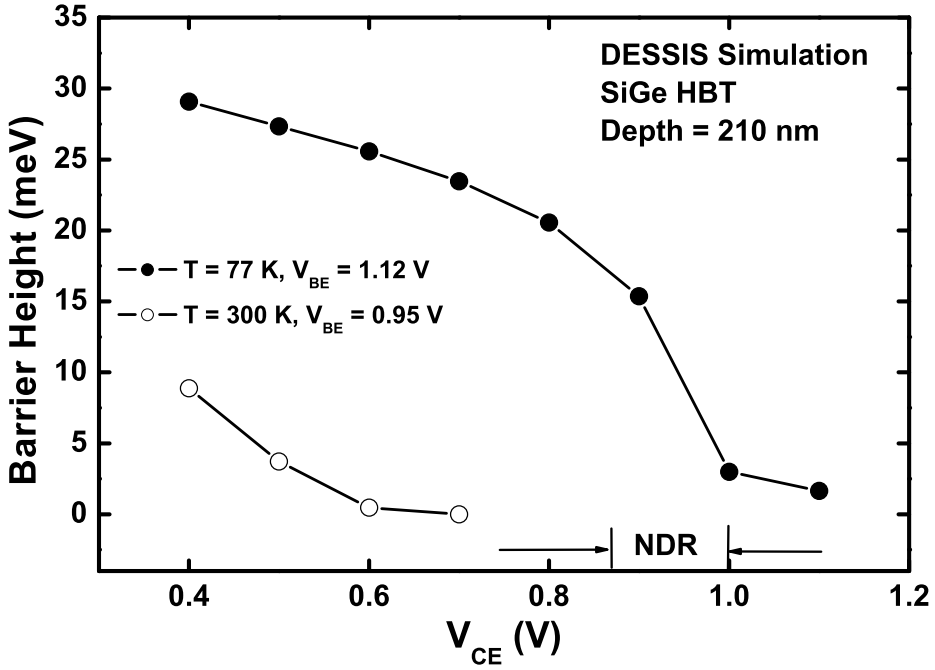

Figure 19: Simulated heterojunction barrier height as a function of V_{CE} for the SiGe HBT at 77K and 300K. The snapshot is taken at the position of the cut line indicated in Figure 12.

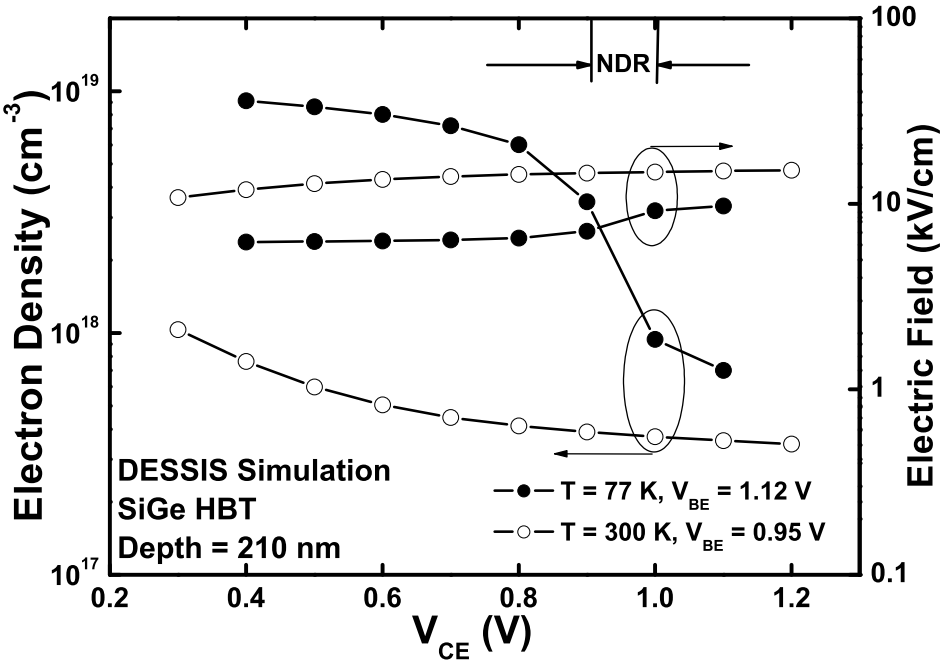

Figure 20: Simulated electron density and electric field as functions of V_{CE} for the SiGe HBT at 77K and 300K. The snapshot is taken at the position of the cut line indicated in Figure 12.

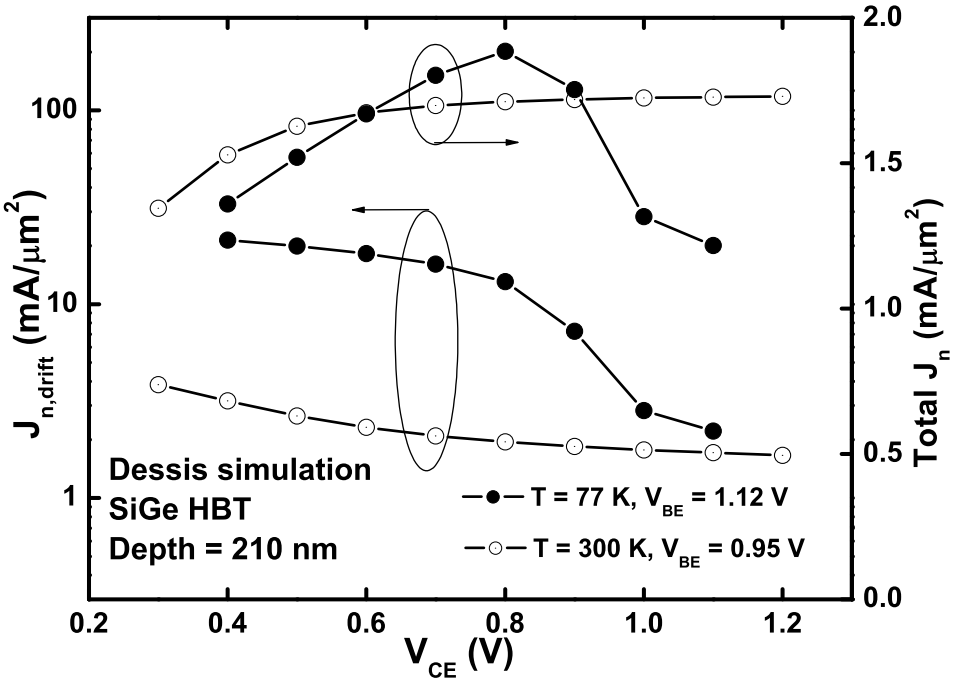

Figure 21: Simulated drift component of the electron current density and the total electron current density as functions of V_{CE} for the SiGe HBT at 77K and 300K. The snapshot is taken at the position of the cut line indicated in Figure 12.

CHAPTER 5

DISCUSSION

5.1 *ac* Consequences

These novel effects also influence the *ac* performance of the device at cryogenic temperatures. In contrast to the situation at 300 K, where f_T decreases monotonically with increasing I_C above peak f_T, the extra accumulation of charges in the base due to HBE at cryogenic temperatures causes an unusual "dip" in the f_T-I_C characteristics (Fig. 22). That is, the *ac* degradation is larger than one would otherwise expect, and partially offsets the generally favorable impact of cooling on SiGe HBT dynamic performance. Fortunately, however, for most circuit applications, this dip occurs well above operational bias current densities.

5.2 Collector Doping and Technology Scaling

To quantitatively investigate the influence of collector doping and technology scaling, a normalized transconductance per unit current parameter (g'_m), which can be easily extracted from the Gummel characteristics of the device, and is defined as,

$$g'_m = \frac{g_{m,peak}}{I_{C,barrier}} \tag{8}$$

where $g_{m,peak}$ is the peak g_m value in the g_m spike (using a V_{BE} step of 2 mV) and $I_{C,barrier}$ stands for the threshold collector current at which HBE turns on. Substituting (6) and (7) into (8), one obtains,

$$g'_m = \frac{1}{I_{C,barrier}} \cdot \frac{\partial I_C}{\partial V_{BE}} = \frac{1}{I_{C,barrier}} \cdot (\frac{\partial I_n}{\partial V_{BE}} + \frac{\partial I_p}{\partial V_{BE}}) \tag{9}$$

Consequently,

$$g'_m = \frac{1}{J_{C,barrier}} \cdot \frac{\partial \left[q \cdot \mu_n \cdot n \cdot E + q \cdot \mu_n \cdot \nabla \left(\frac{nkT}{q} \right) + J_p \right]}{\partial V_{BE}} \tag{10}$$

Or,

$$g'_m \approx \frac{1}{J_{C,barrier}} \cdot \frac{\partial (q \cdot \mu_n \cdot n \cdot E)}{\partial V_{BE}} = \frac{1}{n} \cdot \frac{\partial n}{\partial V_{BE}} + \frac{1}{E} \cdot \frac{\partial E}{\partial V_{BE}} \tag{11}$$

At the onset of HBE at deep cryogenic temperatures, $\frac{1}{E} \cdot \frac{\partial E}{\partial V_{BE}} \ll \frac{1}{n} \cdot \frac{\partial n}{\partial V_{BE}}$ because of the enhanced positive feedback that rapidly accumulates electrons in the base. As a result, (11) can then be simplified as,

$$g'_m \approx \frac{1}{n} \cdot \frac{\partial n}{\partial V_{BE}}|_{V_{BE}=V_{BE,barrier}} \tag{12}$$

where $V_{BE,barrier}$ is the V_{BE} at which HBE turns on. Therefore, g'_m represents a useful parameter that quantifies the greatly enhanced charge accumulation due to barrier effect, and enables a comparison among different devices or in principle even different technology nodes, independent of parameters such as electron velocity, doping profile, and the depth of SIC region, all of which are strongly profile dependent and typically unknown.

The impact of the collector doping on these HBE-induced cryogenic effects can be experimentally investigated by comparing the high-performance (HP) SiGe HBT with its high-breakdown (HB) SiGe HBT counterpart, both of which exist side-by-side on the same wafer, because the only difference between these two devices lies in the lower collector doping level of the HB device (i.e., the Ge profile is the same). The g_m and the I_C characteristics of the 1^{st}-generation HP and HB SiGe HBTs are shown in Fig. 23, and g'_m are shown in the upper two curves of Fig. 25. The lower collector doping of a HB device yields an earlier onset of both the classical Kirk effect and HBE, and thus is naively expected to have a larger impact on the device Gummel characteristics at low temperatures. Therefore, the HB device with a lower SIC doping is expected to show a larger g'_m than the HP device, in agreement with the data.

With regard to technology scaling, the I_C kink effect and the g_m spike also exist in both 3^{rd}-generation (f_T = 200 GHz at 300 K) and state-of-the-art 4^{th}-generation prototype (f_T = 350 GHz at 300 K) SiGe HBTs operating at deep cryogenic temperatures (Fig. 24), but the impact is suppressed in magnitude compared to that in 1^{st}-generation SiGe HBTs.

In fact, the g_m spike in the 4^{th}-generation SiGe HBT is only observable at extremely low temperatures (< 10 K). Additionally, the NDR in the forced-V_{BE} output characteristics is entirely buried by the increasing electron velocity with the increase of V_{CE}, and cannot be clearly observed, even at 5.4 K. The suppression of these effects with technology scaling is expected, given that the collector regions of the scaled transistors are naturally much more heavily doped, partially mitigating HBE and its impact on device performance.

Fig. 25 summarizes the g'_m of the 1^{st}-, 3^{rd}-, and 4^{th}-generation HP SiGe HBTs and the 1^{st}-generation HB SiGe HBTs, highlighting this trend of suppression with the advancement in device speed and technology node. In addition, one can see from the figure that higher V_{CB} causes lower g'_m as HBE is suppressed at higher CB bias. One can thus conclude that the charge accumulation due to the positive feedback in HBE at cryogenic temperatures can be suppressed as long as the HBE is mitigated by higher SIC doping, higher CB bias, and careful technology scaling. This is clearly good news.

5.3 Circuit Implications

From a circuit application perspective, the NDR effect observed here is operative only in the constant-voltage input bias mode, not in the constant-current input bias mode. Traditionally, however, circuit designers rarely worry about the differences between the constant-current input and constant-voltage input modes of operation for bipolar transistors. Either set of output characteristics, regardless of forced-I_B or forced-V_{BE} bias, is typically regarded as sufficient for understanding circuit design [54], [55]. While a difference in Early voltage with respect to the two different modes of operation was reported in [56] for Si BJTs, more serious circuit-relevant concerns were highlighted by *Joseph et al.*, who reported the influence of neutral base recombination on the temperature dependence of Early voltage in SiGe HBTs [57].

There are in fact circuit-relevant examples which invoke a forced-I_B or a forced-V_{BE} mode of operation of the transistors, including high-source resistance current sources and

low-source resistance current sources [57]. In reality, most circuits in real applications operate in a state lying somewhere between these two extremes – that is, they are not driven by an ideal current source or an ideal voltage source, but something in between. Equivalently, a series resistance $R_{B,series}$ can be connected between the base and the voltage source. The constant-voltage input mode is then represented by $R_{B,series} = 0$, while the constant-current input mode is represented by $R_{B,series} = \infty$, the two extremes of most practical circuits.

For better understanding of how the present NDR potentially could affect real circuit designs, a complete set of output characteristics were measured using the circuit configuration shown in the inset of Fig. 27. The output characteristics gradually approach the pure forced-I_B output characteristics, and the NDR weakens as $R_{B,series}$ increases from 0 to 2 kΩ (Fig. 27). One can also observe that the NDR almost disappears when $R_{B,series} = 2\ k\Omega$. Quantitatively, the associated ECR decays exponentially with $R_{B,series}$, as shown in Fig. 28, which can be modeled as,

$$ECR\,(R_{B,series}) = ECR_0 + B \cdot e^{(-R_{B,series}/R_0)} \tag{13}$$

where the fitting parameters $ECR_0 = 0.0095$, $B = 0.1665$, and $R_0 = 449.1\Omega$.

The output impedance of the previous stage of the circuit or the internal resistance of a voltage source can be regarded as $R_{B,series}$ in real circuits and can obviously have a strong influence on the magnitude of the HBE-induced NDR effect. Circuit designers worried about such effects should incorporate the output impedance of their input circuit into their designs to carefully assess the impact of these novel NDR effects. Resultant NDR-induced circuit instabilities, in this context, may indeed be of concern to circuits biased in this region, and potential circuits of concern would include the output stages of analog circuits, current sources, and high-current drivers. Careful compact modeling is obviously warranted, and we note that existing compact models for SiGe HBTs (e.g., VBIC, MEXTRAM, or HICUM) do not at present account for such unique NDR effects. Convergence issues need to be carefully addressed.

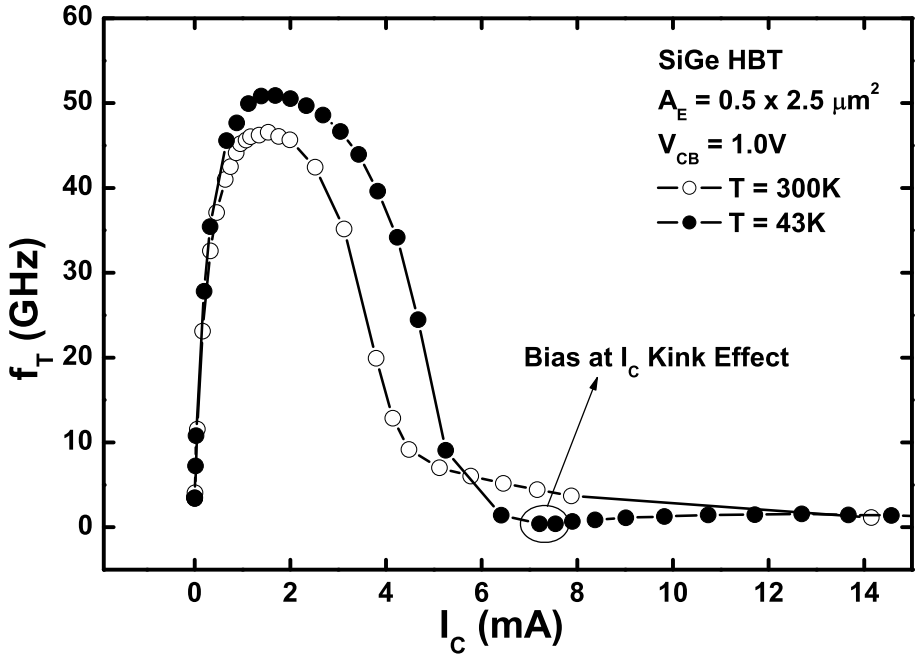

Figure 22: Measured cut-off frequency (f_T) *vs.* collector current (I_C) for the SiGe HBT at 77K and 300K. The 77K plot shows an f_T "dip" in accordance with the I_C kink effect in its *dc* characteristics.

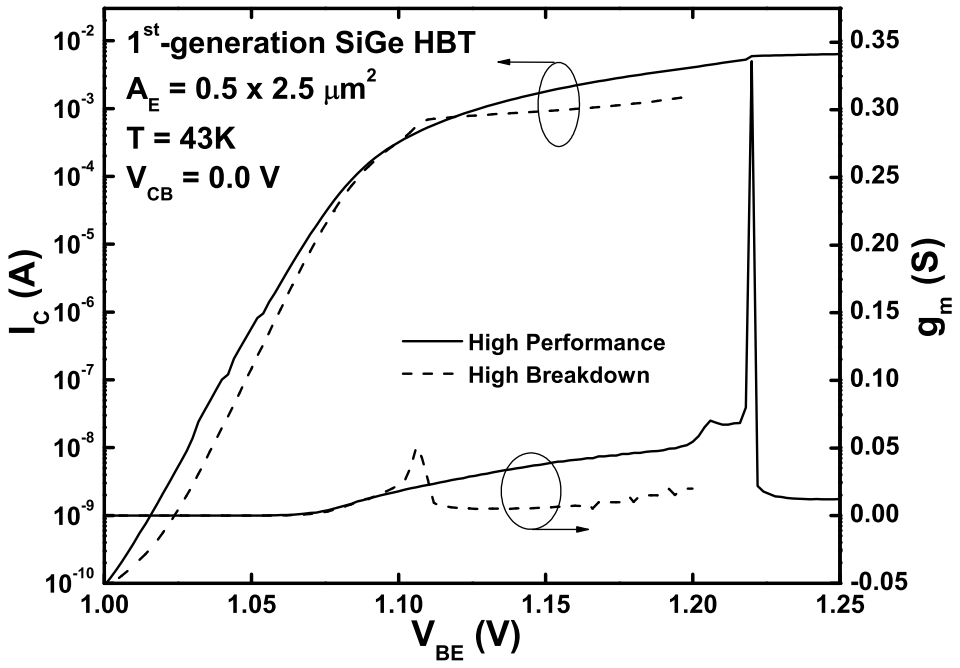

Figure 23: Measured Gummel characteristics and transistor transconductance (g_m) at V_{CB} = 0 V for the HB and HP first-generation SiGe HBTs at 43 K.

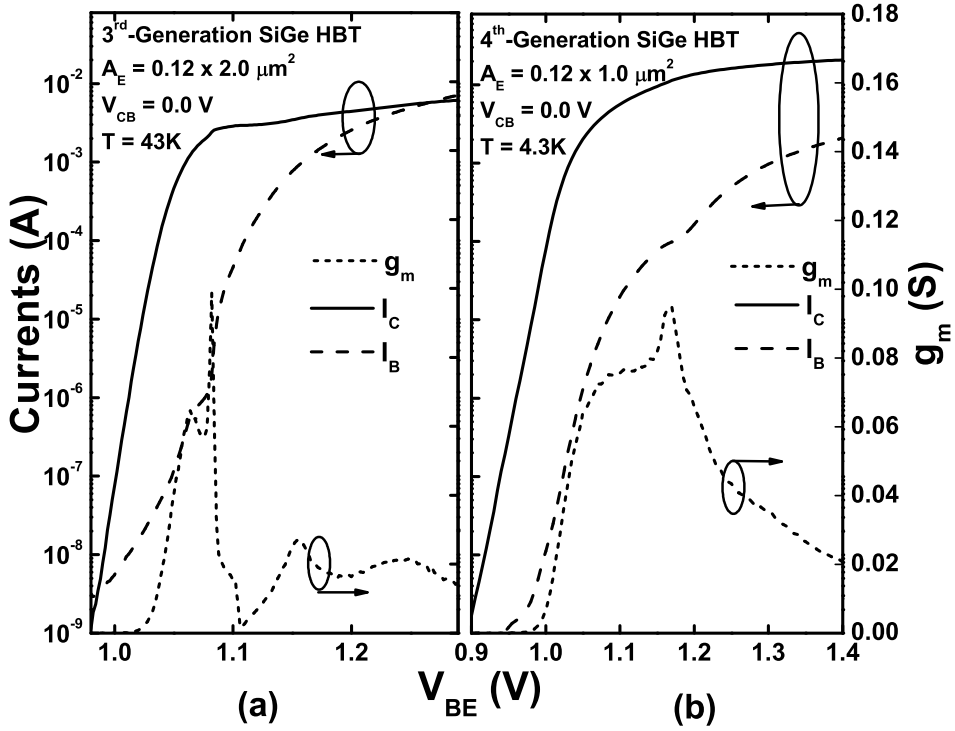

Figure 24: Measured Gummel characteristics and transistor transconductance (g_m) at V_{CB}=0V for (a) 3^{rd}-generation SiGe HBT (200 GHz at 300K) at 43K, and (b) 4^{th}-generation SiGe HBT (350 GHz at 300K) at 4.3K.

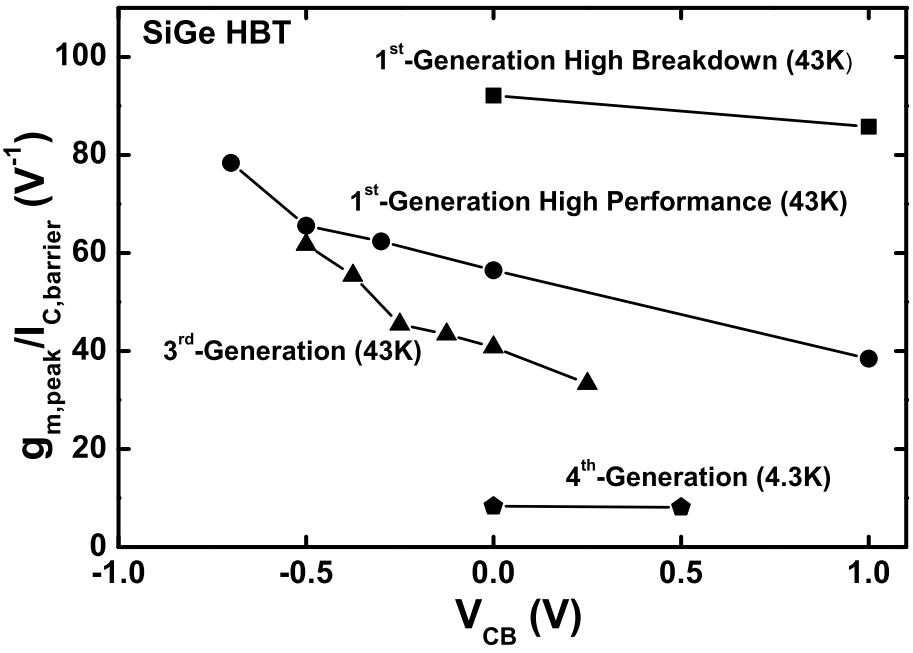

Figure 25: Measured peak unit transconductance (g'_m) as a function of V_{CB} for the first- (both HP and HB), third-, and fourth-generation SiGe HBTs.

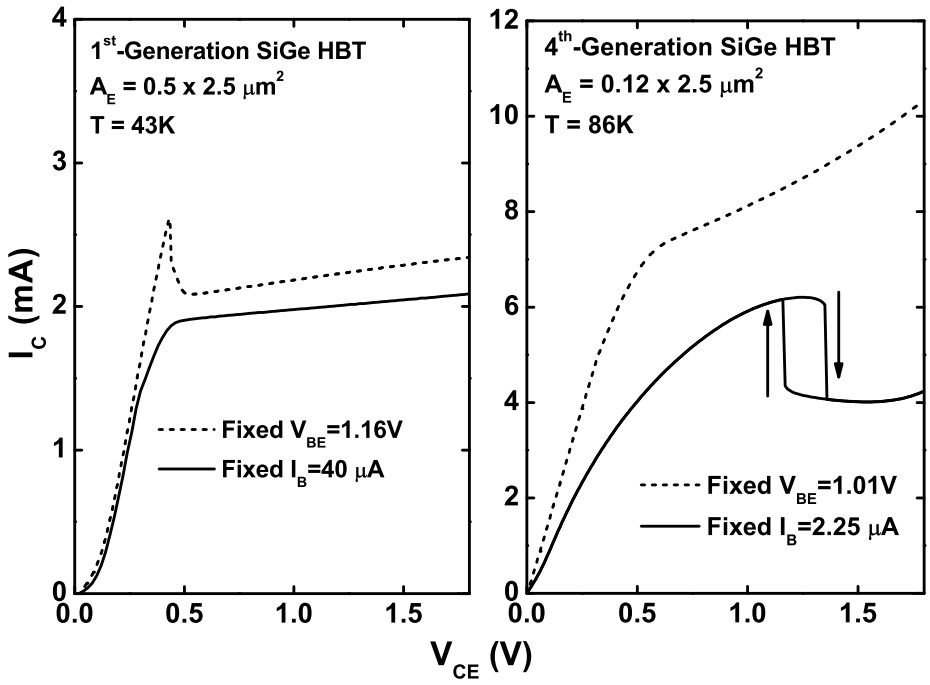

Figure 26: Comparison of the different NDR effects in the 1^{st}-generation and the state-of-the-art 4^{th} generation SiGe HBTs. NDR is observed in the forced-V_{BE} output characteristics of the 1^{st}-generation SiGe HBTs, but in the forced-I_B output characteristics of the 4^{th}-generation devices together with a hysteresis behavior.

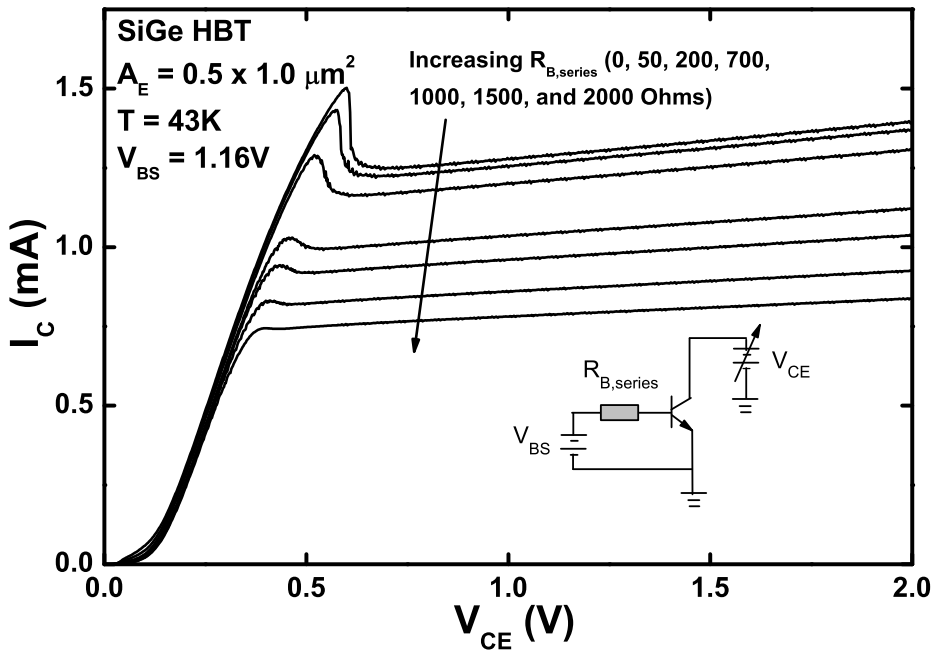

Figure 27: The measured forced-V_{BE} output characteristics of SiGe HBT at 43K and at V_{BS}=1.16V by changing the value of the base series resistance.

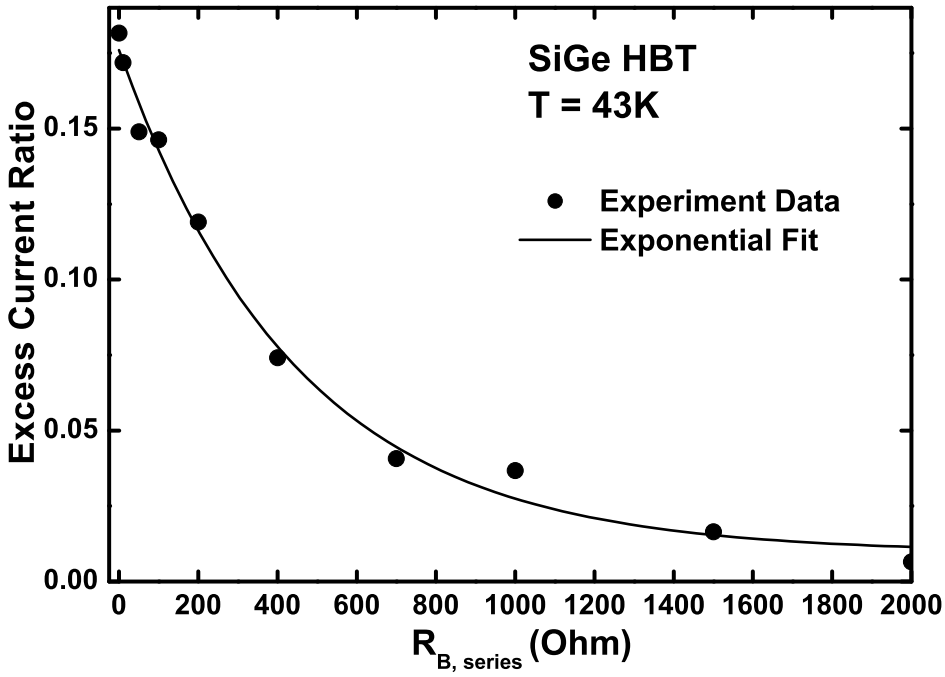

Figure 28: The measured excess current ratio at 43K as a function of the base series resistance.

CHAPTER 6

CONCLUSIONS

A detailed investigation of a new NDR effect and a novel collector-current kink effect in cryogenically-operated SiGe HBTs has been presented in this thesis. It has been shown that the additional drift current due to the charge accumulation induced by the enhanced positive feedback in HBE causes these effects. 2-D DESSIS simulations are used to confirm the proposed mechanism. The enhanced positive feedback at extremely low temperatures influences the *ac* performance of the device by producing an f_T "dip" in the $f_T - I_C$ characteristics. Technology scaling is shown to partially mitigate these effects. These novel effects are also compared to recently-reported NDR and hysteresis effects in the state-of-the-art SiGe HBTs. Circuit designers working in these environmental regimes should pay close attention to potential NDR-induced instabilities.

References

[1] J. Yuan, C. Zhu, Y. Cui, J.D. Cressler, G. Niu, Q. Liang, E. Zhao, A. Appaswamy, R. Krithivasan, and A. Joseph, "A New Device Phenomenon in Cryogenically-Operated SiGe HBTs," *Tech. Dig. of the Int. Electron Devices Meeting,* pp. 611-614, 2006.

[2] J. Yuan, J. D. Cressler, C. Zhu, Y. Cui, G. Niu, Q. Liang, and A. J. Joseph, "An investigation of negative differential resistance and novel collector current kink effects in SiGe HBTs operating at cryogenic Temperatures," *IEEE Trans. on Electron Devices*, vol. 54, pp. 504-516, 2007.

[3] D. L. Harame, D. C. Ahlgren, D. D. Coolbaugh, J. S. Dunn, G. G. Freeman, J. D. Gillis, R. A. Groves, G. N. Hendersen, R. A. Johnson, A. J. Joseph, S. Subbanna, A. M. Victor, K. M. Watson, C. S. Webster, and P. J. Zampardi, "Current status and future trends of SiGe BiCMOS technology," *IEEE Trans. Electron Devices*, vol. 48, pp. 2575-2594, 2001.

[4] J. S. Rieh, B. Jagannathan, D. R.Greenberg, M. Meghelli, A. Rylyakov, F. Guarin, Z. Yang, D. C. Ahlgren, G. Freeman, P. Cottrell, and D. Harame, "SiGe heterojunction bipolar transistors and circuits toward terahertz communication applications," *IEEE Trans. Microwave Theory and Techniquies*, vol. 52, pp, 2390-2407, 2004.

[5] M. Khater, J. -S. Rieh, T. Adam, A. Chinthakindi, J. Johnson, R. Krishnasamy, M. Meghelli, F. Pagette, D. Sanderson, C. Schnabel, K. T. Schonenberg, P. Smith, K. Stein, A. Stricker, S. -J. Jeng, D. Ahlgren, and G. Freeman, "SiGe HBT Technology with f_{max}/f_T = 350/300 GHz and Gate Delay Below 3.3 ps," *Tech. Dig. of the Int. Electron Devices Meeting,* pp. 247-250, 2004.

[6] J. D. Cressler, "On the potential of SiGe HBTs for extreme environment electronics," *Proceedings of the IEEE*, vol. 93, pp. 1559-1582, 2005.

[7] J. D. Cressler, R. Krithivasan, G. Zhang, G. Niu, P. Marshall, H. Kim, R. Reed, M. Palmer, and A. Joseph, "An investigation of the origins of the variable proton tolerance in multiple SiGe HBT BiCMOS technology generations,," *IEEE Trans. on Nuclear Science*, vol. 49, pp. 3203-3207, 2002.

[8] Y. Lu, J. D. Cressler, R. Krithivasan, Y. Li, R. A. Reed, P. W. Marshall, C. Polar, G. Freeman, and D. Ahlgren, "Proton tolerance of third-generation 0.12 μm 185 GHz SiGe HBTs," *IEEE Trans. on Nuclear Science*, vol. 50, pp. 1811-1815, 2003.

[9] J. D. Cressler, J. H. Comfort, E. F. Crabbe, G. L. Patton, J. M. C. Stork, J. Y. -C. Sun, and B. S. Meyerson, "On the profile design and optimization of epitaxial Si- and SiGe-base bipolar technology for 77 K applications. I. transistor DC design considerations," *IEEE Trans. on Electron Devices*, vol. 40, pp. 525-541, 1993.

[10] B. Banerjee, S. Venkataraman, Y. Lu, Q. Liang, C. -H. Lee, S. Nuttinck, D. Heo, Y. -J. Chen, J. D. Cressler, J. Laskar, G. Freeman, and D. C. Ahlgren, "Cryogenic operation of third-generation, 200-GHz peak-f_T, silicon-germanium heterojunction bipolar transistors," *IEEE Trans. on Electron Devices*, vol. 52, pp. 585-593, 2005.

[11] D. L. Harame, J. H. Comfort, J. D. Cressler, E. F. Crabbe, J. Y. -C. Sun, B. S. Meyerson, and T. Tice, "Si/SiGe epitaxial-base transistors. I. materials, physics, and circuits," *IEEE Trans. on Electron Devices*, vol. 42, pp. 455-468, 1995.

[12] A. J. Joseph, J. D. Cressler, and D. M. Richey, "Operation of SiGe heterojunction bipolar transistors in the liquid-Helium temperature regime," *IEEE Electron Device Letters*, vol. 16, pp. 268-170, 1995.

[13] R. Krithivasan, Y. Lu, J. D. Cressler, J. -S. Rieh, M. H. Khater, D. Ahlgren, and G. Freeman, "Half-Terahertz Operation of SiGe HBTs," *IEEE Electron Device Letters*, vol. 27, pp. 567-569, 2006.

[14] Q. Liang, R. Krithivasan, A. Ahmed, Y. Lu, Y. Li, J. D. Cressler, G. Niu, J. -S.Rieh, G. Freeman, D. Ahlgren, and A. Joseph, "Analysis and understanding of unique cryogenic phenomena in state-of-the-art SiGe HBTs," *Solid State Electronics*, vol. 50, pp. 964-972, 2006.

[15] J. Yuan, C. Zhu, Y. Cui, J.D. Cressler, G. Niu, Q. Liang, E. Zhao, A. Appaswamy, R. Krithivasan, and A. Joseph, "A New Device Phenomenon in Cryogenically-Operated SiGe HBTs," *Tech. Dig. of the Int. Electron Devices Meeting,* to be presented, 2006.

[16] S. Tiwari, "A new effect at high currents in heterostructure bipolar transistors," *IEEE Electron Device Letters*, vol. 9, pp. 142-144, 1988.

[17] S. Tiwari and D. J. Frank, "Analysis of the operation of GaAlAs/GaAs HBTs," *IEEE Transactions on Electron Devices*, vol. 36, pp. 2105¿C2121, 1989.

[18] Z. Yu, P. E. Cottrell, and R. W. Dutton, "Modeling and simulation of high-level injection behavior in double heterojunction transistors," in *Proc. IEEE Bipolar/BiCMOS Circuits and Technology Meeting*, pp. 192-194, 1990.

[19] J. D. Cressler, D. M. Richey, R. C. Jaeger, E. F. Crabe, J. H. Comfort, and J. M. C. Stock, "High-injection barrier effects in SiGe HBTs operating at cryogenic temperatures," *Journal De Physics IV*, vol. 4, pp. C6-117 - C6-122, 1994.

[20] A. J. Joseph, J. D. Cressler, D. M. Richey, and G. Niu, "Optimization of SiGe HBT's for operation at high current densities," *IEEE Transactions on Electron Devices*, vol. 46, pp. 1347-1354, 1999.

[21] Q. Liang, J. D. Cressler, G. Niu, R. M. Malladi, K. Newton, and D. L. Harame, "A physics-based high-injection transit-time model applied to barrier effects in SiGe HBTs," *IEEE Trans. on Electron Devices*, vol. 49, pp. 1807-1813, 2002.

[22] B. K. Ridley and T. B. Watkins, "The possibility of negative resistance effects in semiconductors," *Proceedings of the Physical Society*, vol. 78, pp. 293-304, August 1961.

[23] C. Hilsum, "Transferred electron amplifiers and oscillators,' *Proc. IRE,* vol. 50, pp. 185-189, February 1962.

[24] D. E. McCumber and A. G. Chynoweth, "Theory of negative-conductance amplification

and of Gunn instabilities in 'two-valley' semiconductors," *IEEE Transactions*

on Electron Devices,, vol. ED-13, January 1966.

[25] B. K. Ridley and T. B. Watkins, "The dependence of capture rate on electric field and the possibility of negative resistance in semiconductors," *Proceedings of the Physical Society,* vol. 78, pp. 710-715, November 1961

[26] B. K. Ridley and R. G. Pratt, "A bulk differential negative resistance due to electron tunnelling through an impurity potential barrier," *Physics Letters,* vol. 4, pp. 300-302, May 1963,

[27] J. J. O'Dwyer, "Theory of Double Charge Ejection from a Dielectric", *Journal of Applied Physics*, vol. 39, pp. 4356-4359, August 1968.

[28] L. Esaki, "New phenomenon in narrow germanium P-N junctions", *Physical Review*, vol. 109, pp. 603-604, January 1958.

[29] L. L. Chang, L. Esaki, R. Tsu, "Resonant tunnelling in semiconductor double barriers," *Applied Physics Letters*, vol. 24, pp. 593-595, June 1974.

[30] D. H. Chow, T. C. McGill, I. K. Sou, J. P. Faurie, and C. W. Nieh, "Observation of negative differential resistance from a single barrier heterostructure", *Applied Physics Letters,*

vol. 52, pp.54-56, January 1988.

[31] H. Munekata, T. P. Smith, and L. L. Chang, "Growth and transport properties of (Ga,Al)Sb barriers on InAs," *Journal of Vacuum Science and Technology B (Microelectronics Processing and Phenomena),* vol. 72, pp. 324-326, 1989.

[32] J. R. Soderstrom, D. H. Chow, and T.C. McGill, "New negative resistance device based on resonant interband tunneling," *Applied Physics Letters*, vol. 55, pp. 1094-1096, November 1989.

[33] P. See, D. J. Paul, B. Hollander, S. Mantl, I. V. Zozoulenko, and K. F. Berggren, "High performance Si/$Si_{1-x}Ge_x$ resonant tunneling diodes," *IEEE Electron Device Letters*, vol. 22, pp. 182-184, 2001.

[34] F. Capasso, S. Sen, F. Beltram, L. M. Lunardi, A. S. Vengurlekar, P. R. Smith, N. J. Shah, R. J. Malik, and A. Y. Cho, "Quantum functional devices: resonant-tunneling transistors, circuits with reduced complexity, and multiple-valued logic," *IEEE Transactions on Electron Devices,* vol. 36, pp. 2065-2082.

[35] A. Cidronali, G. Collodi, M. Camprini, V. Nair, G. Manes, J. Lewis, and H. Goronkin, "Ultra low-power VCO based on InP-HEMT and heterojunction interband tunnel diode for wireless application," *Tech. Dig. of IEEE RF IC Symp.,* pp. 297-300, 2002.

[36] T. P. E. Broekaert, B. Brar, J. P. A. van der Wagt, C. Seabaugh, T. S. Moise, and F. J. Morris, "A monolithic 4-bit 2-Gsps resonant tunneling analog-to-digital converter," *IEEE Journal of Solid State Circuits,* vol. 33, pp.1342-1349, 1998.

[37] S. J. Wei, H. C. Lin, R. C. Potter, and D. Shupe, "A self-latching A/D converter using resonant tunneling diodes," *IEEE Journal of Solid State Circuits*, vol. 28, pp697-700, 1993.

[38] A. Miura, T. Yakihara, S. Uchida, S. Oka, S. Kobayashi, H. Kamada, "Monolithic sampling head IC," *IEEE Transactions on Microwave Theory and Technology*, vol. 38, pp.1980-1985, 1990.

[39] K. Arai, H. Matsuzaki, K. Maezawa, T. Otsuji, T. Yamamoto, "Static frequency divider featuring reduced circuit complexity by utilizing resonant tunneling diodes in combination with HEMTs," *IEEE Electron Device Letters,* vol. 18, pp.544-546, 1997.

[40] S. -Y. Chung, S. -Y. Park, J. W. Daulton, R. Yu, P. R. Berger and P. E. Thompson, "Integration of Si/SiGe HBT and Si-based RITD demonstrating controllable negative differential resistance for wireless applications", *Solid-State Electronics*, vol. 50, pp. 973-978, 2006.

[41] R. Duane, A. Mathewson, and A. Concannon, "Bistable gated bipolar device," *IEEE Electron Device Letters,* vol. 24, pp. 661-663, 2003.

[42] X. Cheng and R. Duane, "A comprehensive study of bistable-gated-bipolar device," *IEEE Transactions on Electron Devices*, In press.

[43] K. Ismail, B. S. Meyerson, and P. J. Wang, "Electron resonant tunneling in Si/SiGe double barrier diodes," *Applied Physics Letters,* vol. 59, pp. 973-975, 2000.

[44] M. W. Dashiell, R. T. Troeger, S. L. Rommel, T. N. Adam, P. R. Berger, C. Guedj, J. Kolodzey, A. C. Seabaugh, R. Lake, "Current-voltage characteristics of high current density silicon Easki diodes grown by molecular beam epitaxy and the influence of thermal annealing," *IEEE Transactions on Electron Devices*, vol. 47, pp. 1707-1714, 2000.

[45] D. C. Ahlgren, M. Gilbert, D. Greenberg, S. J. Jeng, J. Malinowski, D. Nguyen-Ngoc, K. Schonenberg, K. Stein, R. Groves, K. Walter, G. Hueckel, D. Colavito, G. Freeman, D. Sunderland, D. L. Harame, and B. Beyerson, "Manufacturability demonstration of an integrated SiGe HBT technology for the analog and wireless marketplace," *Tech. Dig. of the Int. Electron Devices Meeting,* pp. 859-862, 1996.

[46] B. Jagannathan, M. Khater, F. Pagette, J. -S. Rieh, D. Angell, H. Chen, J. Florkey, F. Golan, D. R. Greenberg, R. Groves, S. J. Jeng, J. Johnson, E. Mengitsu, K. T. Schonenberg, C. M. Schnabel, P. Smith, A. Stricker, D. Ahlgren, G. Freeman, K. Stein, and S. Subanna, "Self-aligned SiGe NPN transistors with 285 GHz f_{max} and 207 GHz f_T in a manufacturable technology," *IEEE Electron Device Letters*, vol. 23, pp. 258-260, 2002.

[47] J. -S. Rieh, B. Jagannathan, H. Chen, K. T. Schonenberg, D. Angell, A. Chinthakindi, J. Florkey, F. Golan, D. Greenberg, S. -J. Jeng, M. Khater, F. Pagette, C. Schnabel, P. Smith, A. Stricker, K. Vaed, R. Volant, D. Ahlgren, G. Freeman, K. Stein, and S. Subbanna, "SiGe HBTs with cut-off frequency of 350GHz," *Tech. Dig. of the Int. Electron Devices Meeting,* pp. 771-774, 2002.

[48] C. T. Kirk, "Theory of transistor cutoff frequency falloff at high current densities," *Proc. of the IRE,* pp. 164, 1962.

[49] W. M. Webster, "On the variation of junction-transistor current-application factor with emitter current," *Proc. of the IRE,* vol. 42, pp. 914-916, 1954.

[50] E. S. Rittner, "Extension of the theory of the junction transistor," *Physical Review,* vol. 94, pp. 1161-1171, 1954.

[51] J. D. Cressler and G. Niu, *Silicon-Germanium Heterojunction Bipolar Transistors,* Artech House, 2003.

[52] A. Selberherr, "MOS Device modeling at 77K," *IEEE Trans. on Electron Devices*, vol. 36, pp. 1464-1474, 1989.

[53] Q. Liang, R. Krithivasan, A. Ahmed, Y. Lu, Y. Li, J. D. Cressler, G. Niu, J. -S. Rieh, G. Freeman, D. Ahlgren, and A. J. Joseph, "A New Negative-Differential-Resistance Effect in 350GHz SiGe HBTs Operating at Cryogenic Temperatures," *IEEE Int. Solid-State Device Research Conference*, presented December 2005.

[54] P. R. Gray, P. J. Hurst, S. H. Lewis, and R. G. Meyer, *Analysis and design of analog integrated circuits*, Fourth Edition, John Wiley & Sons, 2001.

[55] R. C. Jaeger, *Microelectronic Circuit Design*, McGraw-Hill, 1997.

[56] R. C. Jaeger and A. J. Brodersen, "Self consistent bipolar transistor models for computer simulation," *Solid-State Electronics*, vol. 21, pp. 1269-1272, 1978.

[57] A. J. Joseph, J. D. Cressler, D. M. Richey, R. C. Jaeger, and D. L. Harame, "Neutral base recombination and its influence on the temperature dependence of Early voltage and current gain-Early voltage product in UHV/CVD SiGe heterojunction bipolar transistors," *IEEE Transactions on Electron Devices*, vol. 44, pp. 404-418, 1997.